Thermal Analysis of Water Droplets on PV Panel Surfaces

by Keyur Shah, Bachelor of Science

A Thesis Submitted in Partial
Fulfillment of the Requirements
for the Degree of Master of Science
in the field of Mechanical Engineering

Advisory Committee:

Serdar Celik, Chair

Terry Yan

Kamran Shavezipur

Graduate School
Southern Illinois University Edwardsville
August 2018

ABSTRACT

Thermal Analysis of Water Droplets on PV Panel Surfaces

By

Keyur Jayeshkumar Shah

Chairperson: Serdar Celik

Due to the increasing energy costs and concern on carbon footprint, renewable energy technologies have become more important. Especially after the COP21 Paris meeting, increase in implementation of renewable energy systems has been an important agenda item of countries globally. Among these renewable technologies, solar energy is one of the key players. Hence research on photovoltaic (PV) panels has become more important. Performance of these panels depend not only on the materials science technologies, but also on the operating conditions such as ambient temperature, convective heat transfer, and accumulation of matter such as dust, dirt, snow, or water on the panel surface.

This study investigates the heat transfer effect of water droplets on the panel surface. As surface temperature variation plays a significant role in the efficiency of the solar panel, understanding the heat transfer phenomena between the droplet and the panel is crucial. Temperature variation around the droplet-panel interface was studied both theoretically and numerically. Different cases were studied considering droplet volume, number of droplets, and distance between the droplets. This research concludes that droplet retention on PV panel surface after a rain, condensation or irrigation event is observed when the drag force dominates the body forces. Amount of heat transfer increases with increasing droplet volume and contact area. Hence more heat transfer is observed over hydrophilic surfaces then hydrophobic surfaces. As the number of droplets over the PV panel surface increase, cell temperature

decreases which would yield panel efficiency. It was observed that as the distance between the droplets increases, cooling effect lessens. This decrease in the cooling effect would get higher as the droplets get further away from each other.

ACKNOWLEDGEMENTS

First and foremost, I would like to express my deep and sincere gratitude to my research advisor, Dr. Serdar Celik for giving me the opportunity to conduct research in his team, and providing invaluable guidance throughout this research. His dynamism, vision, sincerity and motivation have deeply inspired me. He is one of the rare professors I have seen who perfectly fits in the Chanakya Niti, which states that “the best teacher is the one who tells you where to look, but does not tell you what to see”. I would also like to thank Dr. Terry Yan and Dr. Kamram Shavezipur for being on my committee and for their valuable time in guiding and evaluating this research.

I am extremely grateful to my lord Shiv for His showers of blessings throughout my studies to complete my research successfully. I am very much thankful to my parents for their sacrifices for educating and preparing me for my future. And last but not least, I am so grateful to all my friends here and back home, who are like a family.

TABLE OF CONTENTS

LIST OF FIGURES

LIST OF TABLES

NOMENCLATURE

A	Cross-section area of the water droplet, m^2
A_F	Projected surface area of the water droplet, m^2
A_{sl}	Real surface area of the water droplet, m^2
C_p	Specific heat at constant pressure, kJ kg^{-1} K^{-1}
D	Diameter of the water droplet at $\theta = 0°$, m
D_r	Diameter of the roughness pillars, m
g	Gravitational force, m s^{-2}
h	Enthalpy, J kg^{-1}
h_c	Heat transfer coefficient, W m^{-1} K^{-1}
i	Internal energy of the control volume, J
k	Thermal conductivity of the material, W m^{-1} K^{-1}
k_r	Retention-force factor, N
k_w	Droplet thermal conductivity W $m^{-1}K^{-1}$
L	Length between the advancing angle to receding angle of droplet, m
P	Pitch distance between roughness pillars, m
P	Pressure, Pa
q'	Heat flux of the control volume, W m^{-2}

Q''' Rate of energy generate per unit volume, J m^{-3}

R Radius of droplet, m

R_f Surface roughness factor

T Temperature, K

t Time, s

T_i Body temperature, K

T_{sat} Water vapor saturation temperature, K

T_∞ Ambient temperature, K

V Volume of the droplet, m^3

V_{PV} Volume of the PV panel, m^3

Greek Symbols

α Condensation coefficient, W $m^{-2}K^{-1}$

β Ratio of length to width of the water droplet

γ Surface tension, N m^{-1}

δ Drop width, m

θ Inclination angle of the surface, °

θ^* Contact angle on rough surface, °

θ_a Advancing angle, °

θ_c	Contact angle on flat surface, °
θ_{cri}	Critical angle of inclination, °
θ_r	Receding angle, °
ρ	Density of the fluid, kg m^{-3}
v	Specific volume, m^3
v_g	Water vapor specific volume, m^3 kg^{-1}

CHAPTER 1

INTRODUCTION

1.1 Concept of PV Panels

Solar energy is in the form of radiation and heat that receives from the sun. Solar energy comes to the earth in the form of light or electromagnetic radiation. Frequency is not same for all electromagnetic waves. X-Rays and UV Rays are most powerful rays with the highest frequency. Solar energy is a means of electromagnetic radiation that can be used for energy generation. But, the solar energy that comes to earth surface also reflected. About 32% of solar energy gets reflected from the surface of the earth. And, remaining solar energy stays in the atmosphere. With the use of photovoltaic (PV) cells, it is possible to absorb electromagnetic rays from solar energy and convert them into another form of energy. Solar energy is one of the biggest sources of renewable energy. Many appliances can directly use this solar energy at home, hospital, school. All appliances convert solar energy into another form of energy by photovoltaic cells. There are two strategies to capture the solar energy, active and passive method. Passive solar heating takes advantage of the exciting heat in the atmosphere. The greenhouse is one of the examples of passive solar heating. When the sun's rays penetrate through the greenhouse, the plants inside the greenhouse absorb the heat and release the heat which provides an environment for the plants to grow. During the winter time, passive solar heating can be used to cut the heating bill. Because passive solar heating does not include any mechanical devices, the proper construction of the house or greenhouse is required. This can be addressed by maximizing amount of the solar light entering the space. Passive solar heating system also depends on the thermal mass of the walls, flooring, and some other structural

components. Thermal mass is the ability of any material to absorbs, store or release the heat. Active solar energy uses mechanical and electrical equipment and converts the heat energy into the different forms of energy. The efficiency of the Active solar heating is much more then Passive solar heating.

Photovoltaics (PV) is energy generation by means of light. PV panels are composed of arrays of cells that contain semiconductors. Semiconductors are usually made of a silicon material. Solar cells have positive and negative junctions (P and N junctions). There is a free electron in the atomic structure of silicon. That free electron gets charge by solar light. But, there is a condition to charge the free electron. Solar light gets divided into three parts based on the wavelength of the light. Ultraviolet light has the wavelength between 10 nm to 380 nm. Visible light has the wavelength between 380 nm to 750 nm. Visible light includes violet (380-450 nm), blue (450-495 nm), green (495-570 nm), yellow (570-590 nm), orange (590-620 nm), red (620-750 nm) colors. And, infrared light has the wavelength between 750-1,000,000 nm. Within the spectrum; ultraviolet light has 45-47%, visible light has approximately 7%, and infrared light has 46-47% span. As only visible light is used to charge the free electrons, visible light is the only source by which the free electron gets excited and produces current.

As discussed, all solar appliances use solar energy and convert that into a different form of energy. High solar energy generates high power output from a photovoltaic cell is not always true. Solar rays contain high infrared radiation, which is the source of heat. Performance of PV panel depends on the amount of light that it captures not on amount of heat it absorbs. The efficiency of PV panel decreases linearly with increase in operating temperature. Standard operating temperature of the PV panel is between 25°C to 45°C. One of the main advantages of the solar energy is that it doesn't harm the atmosphere and it operates with no acoustic noise.

1.2. Problem Statement

The solar cell consists of semiconducting material which is sensitive to changes in temperature. It exhibits higher efficiency when it operates under favorable temperature conditions. As can be seen in Figure 1.1, output power increases as the cell temperature decreases. Maximum power output, open circuit voltage, short circuit current, fill factors and many more electrical parameters of PV cell changes with the varies in the operating temperature. Besides temperature, there are some other factors which have impact on the efficiency of the PV panel, such as; inclination angle of the PV panel, solar cell characteristics, weather condition, packaging factor, dust and etc. Among these, operational cell temperature is the most dominant factor which affects the efficiency of the PV panel [1].

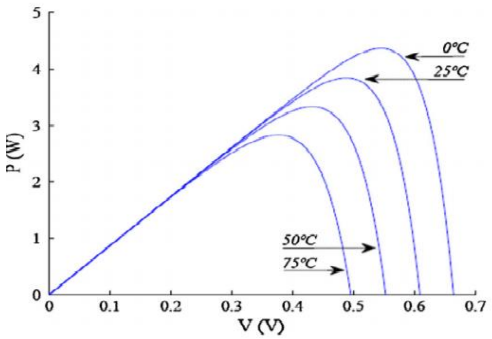

Figure 1.1. Voltage vs temperature graph in PV panel [1]

Jones and Underwood [2] determined the average temperature of PV panel between 27°C – 60°C, when the inclination angle is 30°. They conducted that, in most of the cases when the operating temperature of PV panel passes over 25°C the efficiency of PV panel gets decrease. Each solar cell is in the connection with the other solar cell. When the temperature rises and falls day after day, different expansion and contraction of the connection wire can cause that connection break. Even small impurities like dust and other impurities are always there on the top of the PV panel. To get constant high efficiency, it is very necessary to remove

all those impurities from the PV panel and keep PV panel clean and dust free. Because of the dust layer on PV panel, most of the solar rays gets reflected from the top layer of dust. Hence, solar rays capture photovoltaic cells. In such condition, efficiency of PV panel decreases, yielding higher payback times for consumers.

1.3. Objective of the Study

Water dousing method, or irrigation is one of the most efficient methods to decrease the operating temperature of the PV panels. Following an irrigation, rain, or condensation event some water droplets remain on the surface of the PV panel due to the relation between the adhesive and cohesive forces. This research is focused on the effect of water droplets on the PV panel performance. The main objective of this work is to determine the retention criteria and conditions for the droplets, and to identify the thermal behavior of the droplets on the PV panels, both theoretically and numerically.

CHAPTER 2

LITERATURE REVIEW

In the present time, demand for the energy is continuously increasing. All energy sources have some small or big impact on the environment. Demand for the fossil fuels is continuously increasing day by day. Which increase the amount of the harmful gases like carbon dioxide, methane, nitrous oxide. Today, the most discussed topic is the emission of the carbon dioxide on the environment. Power plants need the huge amount of coal to produce energy. The demand for the fuels also keeps increasing. Over half of the CO_2 comes from the burning of the coals, and one third comes from the burning of the fossil fuels. At present 80% of the total energy generates by the non-renewable resources. For a small country like Bangladesh which has a vast population, it is very important to manage the use of energy in the proper way. Wadud *et al*. [4] conducted a research on the solution to the energy crises in Bangladesh. Where, the demand for the energy is very high because of the large population. To get the solution for energy crises, the people of Bangladesh moves towards the renewable energy. The average rate of daily solar radiation is 4.5-6 kWh/m in Bangladesh which is a good amount of solar radiation. And Bangladesh is also trying to take the advantage of this solar radiation by using various solar systems.

The operating temperature plays a key role in the power generation process of PV panels. Performance of the PV panel depends on the internal and external factors. Internal factors include the material used in PV panel, manufacturing process and many more. External temperature mainly includes the operating temperature and impurities on the PV panel. Dubey *et al.* [5] found out that the efficiency of the PV panel also changes with the latitude. The power

generation rate of PV panel decreases as a decrease in the latitude because of elevated temperature. However, the performance of the PV panel improves at higher altitude. The ambient temperature, local wind speed, solar radiation flux and much more are the factors which may impact on the efficiency of the PV panel. They also carried out the experiment to decrease the operating temperature of PV panel by the air flow on it. They determined that the increase or decrease in temperature of the PV module is much more depends on the speed of the airflow over it, rather than the direction of the air flow. Besides of that, the increase in PV module temperature is more depends on the solar radiation. On an average, only 6-20% of the solar radiation turns in to electrical energy. The remaining solar radiations turn in to heat energy. Tobnaghi *et al.* [6] conducted the effect of temperature on the solar cell efficiency. They measured the efficiency of the PV panel at the different temperature (15°C, 25°C, 30°C, 40°C, 50°C). They measured the efficiency of PV panel at 15°C around 14.63% and at 50°C, 12.25% efficiency. The PV panels gives the best results on the sunny and cold day.

Popovici *et al*. [7] represented a model which increase the efficiency of the PV panel by using an air-cooled heat sink. In which, air flow used to maintain the temperature of the PV panel. They connected the ribs at the back side of the PV panels. The velocity of the air behind the PV panel was set at 1.5 m/s. The angle of the ribs was set at 45°, 90°, and 145° for different cases. At 45°, the highest heat transfer and at 145°, the lowest heat transfer was measured. They concluded that the heat transfer is directly proportional to the height of the ribs and indirectly proportional to the angle of the ribs. Uros and Stritih [8] came up with an idea to increase the efficiency of the PV panel using PCM (Phase change material). The purpose of PCM is to increase the efficiency of the panel by absorbing the excessive heat that is generated by the heating up of the panels. The panels absorb solar radiation and get heated up and the PCM absorbs that excess heats and melts thus keeping PV panel cool.

Although there are various techniques to increase the efficiency of PV Panels, they might not be economical. Poulek *et al.* [9] came up with an idea for cost-effective PV panels. In their experiment, they used PV panels where mirrors are a part of the design. The PV panels are surrounded by mirrors which reflect the radiation onto the panel. This type of system can be highly useful to generate high power output. The drawback of this method is, sometimes because of high radiation, the operating temperature of PV panel reaches at very high point. Matias *et al*. [10] developed the water-cooling technique to maintain the operating temperature of the PV Panel. The cooling process of PV panel by water or air is known as the hybrid method. The hybrid method includes air, water or any other fluid for the cooling operation. They used the water flow to reduce the operating temperature of the PV Panel. The flow rate of the water also plays a major role in the cooling process and the efficiency of the PV Panel. They carried out the experiment under different flow rate of water (4 L/min, 3 L/min, 2 L/min, 1 L/min) to observe the effect of flow rate on the cooling rate. In the results, they found the maximum cooling rate of the PV panel under 2 L/min flowrate of water. The cooling rate of the PV panel at 4 L/min is lower than the cooling rate at 2 L/min. They concluded that the efficiency of the PV panel under the water flow mainly depends on the path of flowing of water, not on the flow rate of the water.

In the desert area, the ambient temperature is very high during the daytime. To keep the temperature of the PV panel low, the amount of the water needed for the cooling process is high. Moharram *et al.* [11] worked to minimize the amount of water for the cooling process by finding the heating and cooling rate model which surmises that, the maximum power output can achieve if the water flow starts when the PV panel temperature reaches at 45°C. Tiwari *et al*. [12] also used the hybrid method to measure the change in cooling rate of the PV panel by using different mechanism. They used glass to glass surface without water flow, glass to tedlar

without water flow, glass to glass with the water flow and glass to tedlar with water flow. Because of the heat transfer rate in the glass is higher than the tedlar so, glass to glass with the water flow model gives the highest efficiency. From above discussion, it is clear that the efficiency of the PV panel is very much depending on the operating temperature. And the hybrid method is a very efficient way to maintain the operating temperature of the PV panel. But the hybrid method is not a cost-efficient method because of high installation cost.

After the rain or hybrid method, there will be a number of the droplets remains on the PV panel because of adhesive force. When there is a temperature difference present between the water droplet and the PV panel at that time those droplets absorb the heat from the PV panel. This heat transfer procedure contributes to control the overall increase of the temperature of PV panel. However, heat transfer only takes place when the water droplet is in the rest condition on the PV panel. Retention of the water droplets on an inclined plane is depend on body force, drag force, gravity force, surface roughness, and many more parameters. Kim *et al.* [13] researched on the sliding velocity of the water droplet on an inclined plane and under what conditions, the water droplet starts moving on an inclined plane. They surmised that the water droplet on an inclined plane starts sliding when the advancing angle of the droplet is more than the inclination angle of the plane and receding angle of the droplet is less than the inclined angle of the plane.

Maurer *et al.* [15] discussed the critical angle for the different volume of the droplets on an inclined plane. Which explains the various conditions under which the droplet changes its stability on an inclined plane. The critical angle is small for the large volume droplet. When all the forces are in the equilibrium condition, there is no change in the geometry of the droplet. The receding part of the droplet starts moving first when the droplets starts sliding on an inclined plane.

Quéré *et al.* [16] did the numerical analysis for the stability of the water droplet on an inclined plane. The capillarity force helps the water droplet to remain on the inclined plane, capillarity force is indirectly proportional to the volume of droplet. Kang and Lee [17] find out the behavior of the liquid droplet on the heated inclined surface which determined that when any droplet comes in contact with the heated plane at that time droplet gets contract and expand serval time before comes in to the rest position.

CHAPTER 3

THEORETICAL ANALYSIS

3.1. Hydrophobicity Effect

After the rain because of adhesive force between water flow and solid surface, water stays on the top of the solar plate in the form of droplets. The shape of the droplet and the stability of the droplet is depending on the cohesive force and adhesive force respectively. Cohesion is sticking together of molecules of the equivalent kind often by hydrogen bonds. The interaction between two water molecules is the type of cohesive force. In water molecule oxygen is more electronegative than the hydrogen and oxygen pulls electrons towards it and acquire a partial negative charge. And hydrogen has a positive charge. Which is the reason for force of attraction occurs which is known as hydrogen bond. Hydrogen bond is a type of cohesive force which connects the water molecules together. Adhesion is the attraction between distinct kinds of molecules. Surface tension is directly related to the intermolecular forces. All molecules attract with each other by cohesive force which creates the surface tension in molecules. The shape of that liquid on the surface depends on the action of adhesive and cohesive force. When the adhesive force is much larger than the cohesive force at that time the water droplet spreads out on the surface and water drop get perfect cylinder shape when the adhesive force is very small.

Shape of any droplet depends on the contact angle with the solid surface. Contact angle measures between solid surface, liquid, and air interaction as shown in figure 3.1. When there is low contact angle between a water droplet and the contact surface (due to high adhesive force) at that time water droplet spreads out and create a very thin layer on the surface. High

contact angle between the water droplet and surface (θ_C > 90°, due to less adhesive force) forms the spherical shape of droplet. Contact angle depends upon the hydrophobicity behavior of surface. Based on the contact angle hydrophobic surface or hydrophilic surface can be determined.

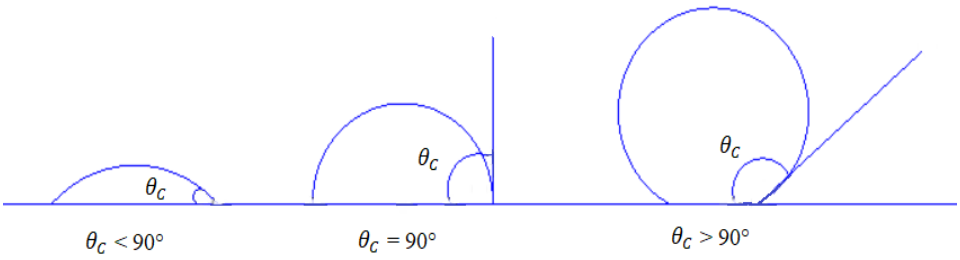

Figure 3.1. Contact angle of liquid droplet on solid plane

High surface energy is the sign of hydrophilic surfaces while hydrophobic surfaces have low surface energy which cannot hold the water droplets. Hydrophilic surface creates the contact angle is less than 90°. Hydrophobic surfaces create the contact angle is greater than 90°. Surface also define as super hydrophobic (θ_C > 150°) and super hydrophilic (θ_C < 5°) [18]. Water on a super hydrophobic surface will roll down and water on super hydrophilic liquid will spread out completely. Force balance on the line of contact gives by Young's equation.

$$\gamma_{sv} - \gamma_{sl} - \gamma_{vl} \cos\theta_C = 0 \tag{3.1}$$

γ_{sv} is surface energy (surface tension) between solid and vapor, γ_{sl} is surface energy between solid and liquid, γ_{vl} is surface energy between vapor and liquid. Equation 3.1 use to determine the contact angle of the droplet at solid-vapor-liquid interphase with the help of surface tension. Surface roughness plays dominant role in hydrophobic or hydrophilic surfaces. Surface roughness can make the hydrophobic surface even more hydrophobic and hydrophilic surface

even more hydrophilic. That decides by, whether the contact is between solid-air-liquid or solid-liquid. Wenzel and Cassie-Baxter create a model which helps to determine the contact angle of the droplet on rough surfaces.

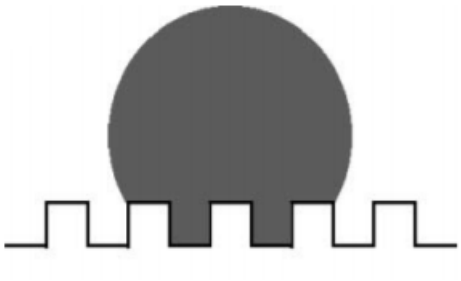

Figure 3.2. Wenzel state of fluid droplet [19]

Wenzel state model is as shown in figure 3.2, the droplet is in complete contact with the surface. Here, droplet actually sticks very well to the solid surface. In Wenzel model, the surface roughness is the ratio of the real surface area to a projected surface area [20].

$$R_f = \frac{A_{sl}}{A_F} \tag{3.2}$$

Since a real surface area is greater than projected surface area in most of the rough surfaces, surface roughness factor always greater than 1. Wenzel equation is given by,

$$\cos\theta^* = R_f \cos\theta_c \tag{3.3}$$

In the equation 3.3, R_f is greater than 1, so $\cos\theta^* > \cos\theta_C$.

If water droplet presents in Cassie-Baxter state at that time water sits on the top of tiny air

bubble as shown in figure 3.3.

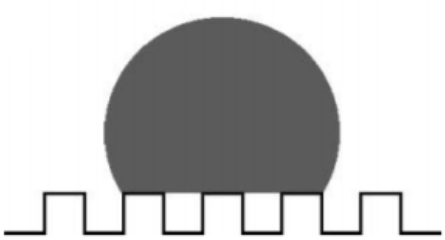

Figure 3.3. Water droplet in Cassie-Baxter state [19]

In this case, when water droplet encounters the solid surface it jumps or rolls off. This phenomenon is useful in the case of self-cleaning of the surface.

Cassie-Baxter state describes by the following equation,

$$\cos\theta^* = -1 + f_{sl}(1 + \cos\theta_C) \tag{3.4}$$

where, f_{sl} is the percentage of solid contacts in a droplet.

In general, on an inclined plane, the advancing angle and the receding angle of the droplet are not same. There are many factors which affect the contact angle hysteresis. The difference between the advancing angle and the receding angle is known as contact angle hysteresis. Bhushan *et al.* [20] give the relation between contact angle (Advancing and Receding contact angle) and contact angle hysteresis. They found that the wetting behavior of surface depends on the surface roughness, size of the roughness pillars and distance between the roughness pillars. Wetting surface area increase with decrease in the surface roughness. They derived a non-dimensional number based on which wetting behavior of the surface figure out. Bhushan *et al.* defined non-dimensional spacing factor.

$$S_f = \frac{D_r}{P} \tag{3.5}$$

Surface roughness is directly proportional to the density of the edges, as edges more on the solid surface then surface roughness increase.

On an inclined plane the forces applied on the droplet in the downwards direction increases with the inclination of surface. Surface roughness plays dominant role in the stability of the droplet on an inclined plane. And when the forces at advancing angle exceed the forces at receding angle at that time the water droplet starts moving in downward direction. velocity gets increase and the water droplet starts making the small sharp angle at the tail as the inclination angle increase. And at high velocity, droplet divided into several small droplets. When water droplet starts moving on a plane at that time it leaves a thin water layer film on the hydrophilic surface.

3.2. Droplet Retention on Inclined Planes

This section concentrates on the study of droplet retention on a smooth inclined surface. This study seeks to understand how droplet shape, advancing angle, receding angle, gravitational force, surface roughness affects the retention of a droplet on an inclined plane. Stability of the droplet, advancing and receding angles can also be predicted by the Bond number. The droplet cannot resist the gravity force at or above some inclination angle and starts sliding on the surface.

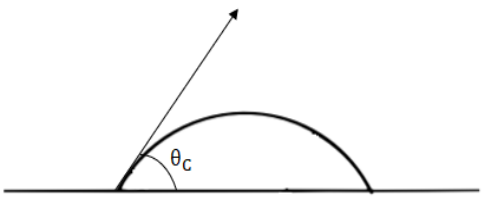

Figure 3.4. Contact angle (θ_C) of the droplet

Water droplet starts forming a new shape with the change in inclination angle. Contact angle helps to determine the shape of a water droplet on the plane. On the horizontal plane, the water droplet has in axis symmetry shape (Receding and Advancing angles are same). But for an inclined plane, the water droplet loses the axis symmetry shape because all the forces are not getting stabilize. Contact angle depends on the surface characteristics and surface tension. Based on the radius of the droplet, surface tension also plays a dominant role to change the size of the water droplet. When the radius of the droplet is less than the capillary radius (2.8 mm for pure water), surface tension affects the shape of the droplet. And the droplet changes its shape into spherical geometry [21]. Most of the raindrops on the plane have a hemisphere shape. Surface tension depends on the volume of the droplet. The pressure in each droplet is different based on the surface tension. Small droplets have very high pressure while big droplet has low pressure. Surface tension also changes with the change in temperature.

Table 3.1. Surface tension with respect to temperature of water

Temperature (°C)	**Surface Tension (10^{-3} N/m)**
5	74.95
10	74.23
15	73.52
20	72.75
25	71.99

When the contact angle is same at the front and back side (on the flat plate) of the droplet at that time, forces at the circular triple boundary is in the equilibrium state. A shape of the droplet gets deform when some external forces applied on the droplet (i.e. gravitational force). When droplet starts moving on the plane at that time opposite force also applies on the

droplet in the reverse direction which is known as the drag force. Drag force depends on the contact area between the water droplet and the surface. The hydrophilic surface has high drag force while hydrophobic surfaces have low drag force.

When the horizontal plane gets inclination at that time, the contact angle at the front (Advancing angle) gets increase and the contact angle at back (Receding angle) gets a decrease. The contact angle hysteresis depends on the inclination angle. The difference in the front and back angle gives rise to retention force (drag force) of the water droplet.

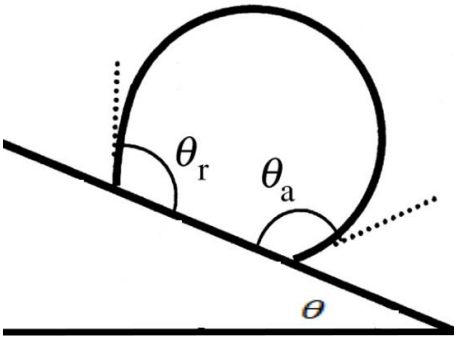

Figure 3.5. Advancing and receding angle of droplet

The inclination angle at which droplet starts sliding down on the plane is known as critical angle (θ_{cri}). When receding angle $\theta_r > 0$ and the inclination angle is more than the critical angle at that time water droplet starts moving downwards. The relation between the inclination angle and contact angle hysteresis can be described as below [18],

$$\rho g A \ \sin\theta = \gamma_{LV}(\cos\theta_r - cos\theta_a) \tag{3.6}$$

For, critical angle of inclination equation (3.6) will be,

$$\rho g A \ \sin\theta_{cri} = \gamma_{LV}(\cos\theta_r - cos\theta_a) \tag{3.7}$$

θ_{cri} is the critical angle of inclination. Here, the right-hand side is the surface tension force and the left-hand side is the gravitation force acting on the water droplet.

The width of the water droplet is in perpendicular direction of the inclination plane. Equation (3.7) can be written as [18],

$$\frac{2\rho g V \sin\theta_{cri}}{\gamma_{LV}} = k_r\, \delta\, (\cos\theta_r - cos\theta_a) \tag{3.8}$$

Where ($\rho g V \sin\theta_{cric}$) is the total force (F) and k_r is the retention-force factor which is equal to 2 (for large contact angle). Retention-force factor (k_r) is not same for all the shapes of the droplet. Retention-force factor (k_r) increases with the elongation of the water droplet. For different droplet k_r can be defined as,

$$k_r = 0.23 + 1.04\,\beta \tag{3.9}$$

Surface roughness also plays a major role in the stability of the water droplet. When there is more surface roughness, water can easily stick to surface. For smooth surfaces, roughness is very less so water can slide easily. When there is a rough surface, water droplet fix into grooves and hills of the surface which can give more friction to water droplet which increases the drag force.

As surface roughness increases, the projected surface area decreases and so the roughness factor increases. Which helps the water droplet to stay on the inclined plane.

$$\frac{2\rho g V \sin\theta_{cri}}{\gamma_{LV}} = k_r\, \delta R_f\, (\cos\theta_r - cos\theta_a) \tag{3.10}$$

where, R_f is the roughness factor.

$$F = \frac{\gamma_{LV}\, k_r\, \delta\, R_f}{2}(\cos\theta_r - cos\theta_a) \tag{3.11}$$

When $F < \gamma_{LV}\, k_r \omega\, R_f (\cos\theta_r - cos\theta_a)$, the water droplet stays in a stable condition. But for, $F \geq \gamma_{LV}\, k_r \omega\, R_f\, (\cos\theta_r - cos\theta_a)$, the water droplet starts sliding on an inclined plane where, $\omega = \frac{\delta}{2}$.

As the volume of the droplet increase, the gravitational force increase. At the same time receding and advancing angles also change. But, change in the retention force $[\gamma_{LV}\, k_r \omega\, R_f (\cos\theta_r - cos\theta_a)]$ is very small (negligible). Because surface tension and retention-force factor do not change much more with increase in the volume of the drop. The critical angle gets decrease as the volume of the droplet increase. With the known value of droplet volume, surface tension and inclination angle, the critical angle of inclination can be finding out. When the water droplet is in rest condition at an angle of inclination θ, Force acting on the droplet is equal to,

$$F = V\rho g \sin\theta \tag{3.12}$$

where, V is volume of the droplet.

On the water droplet, total energy performs by the gravitational force to move the droplet by is equal to,

$$\delta U_g = F\delta x \tag{3.13}$$

Total force needs to move the water droplet by δx is equal to,

$$\delta U_Y = \delta x\ \gamma_{LV} R_f\, \delta\, (1 - \cos\theta_c) \tag{3.14}$$

Water droplet starts moving when gravitational force will be equal to total force needs to move the water droplet ($\delta U_g = \delta U_Y$) . Since $\delta U_g = \delta U_Y$,

$$\sin\theta_{cri} = \frac{\delta\ \gamma_{LV}\ R_f(1-\cos\theta_c)}{\rho g V} \tag{3.15}$$

where, θ_{cri} is the critical angle of inclination. In equation (3.15) critical angle of inclination depends on the contact angle of the water droplet on horizontal surface.

The stability of the droplet also predicted by Bond number. Bond number is the ratio of gravitational force to surface tension force. As gravitational force exceeds the surface tension force, the bond number will be greater than 1 and the droplet gets deform. And if the Bond number less than 1 that means the droplet stays at its same position because surface tension force exceeds the gravitational force.

$$Bo = \frac{\rho g D^2 \sin\theta}{\gamma_{LV}} \tag{3.16}$$

where D is the diameter of the water droplet at 0° inclination angle.

Annapragada *et al.* [23] found the relation between receding angle, advancing angle and Bond number. By this relation, the advancing and receding number can be predicted.

$$\frac{\theta_a}{\theta_c} = 1 + 0.123\ Bo \tag{3.17}$$

$$\frac{\theta_r}{\theta_a} = 1 - 0.298\ Bo \tag{3.18}$$

Similar to the critical angle of inclination, it is also possible to find out the critical volume of the droplet. The water droplet starts sliding on the inclined plane at or above remarkable droplet volume when the inclination angle is constant for the plane. That volume is known as the critical volume of the water droplet. By mathematical derivation, it is possible to find out the relation between the critical volume and the inclination angle of the plane. The contact angle

hysteresis is negligible for a small volume of droplets even if the surface is tilted. In that cases, the droplets form a spherical shape as shown in the figure below,

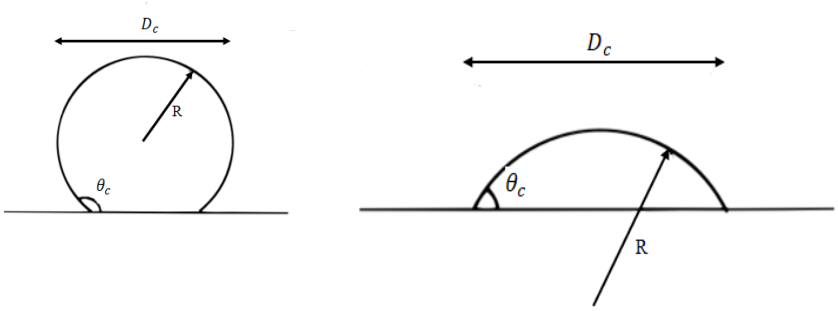

Figure 3.6. Contact diameter and radius of a droplet

Quéré *et al.* [19] defined the volume of the droplet as,

$$V = \frac{\pi}{3} R^3 (2 + \cos\theta_c)(1 - \cos\theta_c)^2 \tag{3.19}$$

In the figure 3.6,

$$D_c = 2R \ \sin\theta \tag{3.20}$$

where, D_c is the contact diameter of the droplet on surface.

$$D_c = \ 2\left(\frac{3}{\pi}\right)^{\frac{1}{3}} \frac{\sin\theta}{(2 + \cos\theta_c)^{1/3}(1 - \cos\theta_c)^{2/3}} \ V^{\frac{1}{3}} \tag{3.21}$$

The relation between the contact diameter and the contact angle can be derived by above equation. When, contact angle is greater then 120°, the diameter is almost constant of a droplet up to 180°. From equation (3.8), it is clear that droplet on inclined plane starts moving when,

$$\frac{2\rho g V \sin\theta_{cri}}{\gamma_{LV}} \geq k_r \ \delta \ (\cos\theta_r - cos\theta_a) \tag{3.22}$$

So,

$$\frac{2\rho g V \sin\theta_{cri}}{\gamma_{LV}\, k_r\, \delta} \geq (\cos\theta_r - cos\theta_a) \tag{3.23}$$

Above equation gives the relationship of contact angle hysteresis and sliding of the water droplet on an inclined plane. Quéré *et al.* [19] derived the maximum contact angle hysteresis above which the droplet starts sliding. Experiments were performed between 5 µl to 25 µl droplet volumes. It was concluded that the maximum contact angle hysteresis above which droplet starts sliding is between 15°-22°, and the average of maximum contact angle hysteresis is 19°.

3.3. Heat Transfer Equation

Heat transfer occurs in the form of conduction between the PV panel and the droplet, and by means of convection between the droplet and the surrounding air. The conduction heat transfer mainly divides in to two parts, first is steady state conduction heat transfer (Temperature is only function of space, not time) and second is unsteady state conduction heat transfer (temperature is function of both time and space). The unsteady state heat transfer also divides in to two parts, which is periodic heat transfer and non-periodic heat transfer. Periodic heat transfer of conduction can be derived by static method or sine-form method. Non-periodic heat transfer of conduction can be derived by Lumped parameter analysis, Heisler chart method and Error function method. The discussion of conduction process always starts with the Fourier's law.

Fourier's law defines the conduction equation as,

$$\frac{dQ}{dt} = -kA\,\frac{dT}{dx} \tag{3.24}$$

The problem observed in this study is unsteady state non-periodic conduction heat transfer. Cooling medium is the water droplet and the energy transfer occurs from the PV panel and air to the water droplet. In the PV panel, heat transfers by conduction and in the water droplet heat transfers by the convection. The PV panel and water droplet both generates conductance resistance and convection resistance respectively.

Conductance resistance is defined as,

$$R_{cond} = \frac{L}{k_s A} \tag{3.25}$$

Convection resistance is defined as,

$$R_{conv} = \frac{1}{h_c A} \tag{3.26}$$

where, h is convective heat transfer co-efficient between the PV panel and water droplet.

Biot number is the ratio of conduction therml resistance to convection thermal resistance, which can be expressed as:

$$Bi = \frac{h_c L}{k_s} \tag{3.27}$$

If Biot number is less than 0.1, lumped parameter analysis becomes handy to solve the problem. On the other hand, for 0.1 < Bi < 100, error function method; and for Bi > 100, Heisler chart method are used, respectively. In the lumped method, the energy balance equation is expressed as:

Rate of decrease of internal energy = (Convection heat transfer between the PV panel) + (water droplet coupling and the surrounding air)

For the problem studied, Biot number was observed to be less than 0.1, enabling the use of lumped capacitance method. The method was applied to the PV panel and droplet coupling, where the coupling interacts with the surrounding air. Hence the relation is given by:

$$-mc_p \frac{dT}{dt} = hA\,(T - T_\infty) \tag{3.28}$$

$$-\rho V_{(PV+Droplet)} c_p \frac{dT}{dt} = hA\,(T - T_\infty) \tag{3.29}$$

Integrating Equation (3.29) with the appropriate boundary conditions yield:

$$\int_{T_0}^{T} \frac{dT}{(T-T_\infty)} = \int_{t=0}^{t} -\frac{hA}{(\rho V_{(PV+Droplet)} c_p)} \tag{3.30}$$

$$\frac{T - T_\infty}{T_i - T_\infty} = exp\left(\frac{hA}{(\rho V_{(PV+Droplet)} c_p)} t\right) \tag{3.31}$$

CHAPTER 4

NUMERICAL ANALYSIS

4.1. Geometry and Meshing

For any numerical analysis, the initial two steps are geometry and meshing of the geometry. The first step is to create the 3-D geometry in the Design Model.

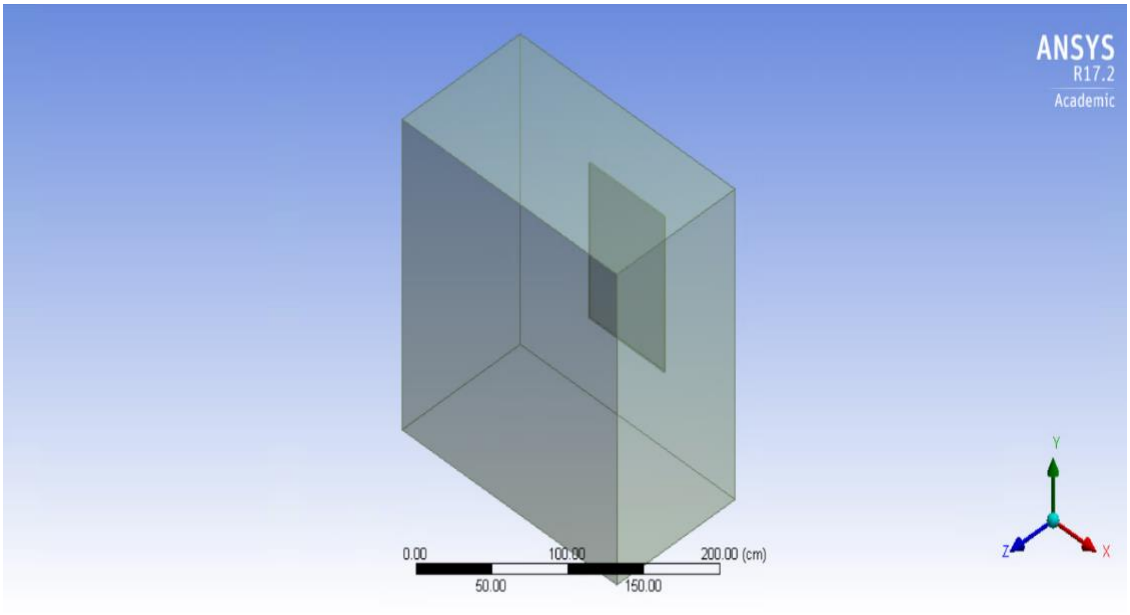

Figure 4.1. Geometry of the model

The geometry for simulation is as shown in Figure 4.1. After the geometry, next and the most crucial step is meshing. The meshing is a very important part of the simulation for the results. Mesh size can be the biggest source of error in the ANSYS analysis. The key to ANSYS analysis is discretization. ANSYS system divides any surface or volume into a number of meshes and computes the solution. The number of nodes increases as mesh size decreases. The accuracy of results improves as the mesh size gets smaller.

Details of "Mesh"	
Export Format	Standard
Shape Checking	CFD
Target Skewness	Program Controlled
Element Midside Nodes	Dropped
Sizing	
Size Function	Curvature
Relevance Center	Fine
Initial Size Seed	Active Assembly
Smoothing	High
Transition	Slow
Span Angle Center	Fine
Curvature Normal Angle	Default (18.0 °)
Min Size	Default (4.3835e-004 m)
Max Face Size	Default (4.3835e-002 m)
Max Tet Size	Default (8.767e-002 m)
Growth Rate	Default (1.20)
Automatic Mesh Based Defeaturing	On
Defeature Size	Default (2.1917e-004 m)

Figure 4.2. Details of mesh

There are also some disadvantages when the small mesh size is in the account. High number of elements takes too much time for simulation. The software takes weeks or months to get the results. Inflection layer is useful to create a precise mesh with a smaller number of nodes. The droplet size is very small compared to the PV panel and problem domain, the temperature distribution near to the water droplet will be high. Far away from the water droplet, the change in temperature will be negligible. Hence, there is no need for a fine mesh all over the geometry. Fine mesh near the droplet however yields results with enhanced accuracy. The objective of inflection layer is to achieve a fine mesh near the area where the heat transfer takes place. The inflection layer is as shown in Figure 4.3.

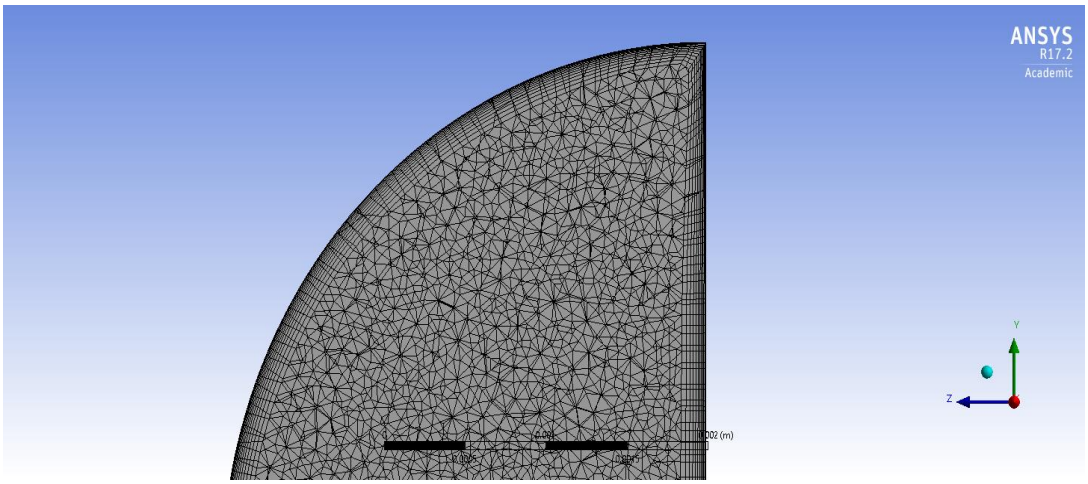

Figure 4.3. Inflection layer in the mesh of a water droplet

To get accurate results different mesh size applied to different bodies. Here, the mesh size of the water droplet, PV plate, and the control volume is different. Mesh size of the water droplet is 9.99e-004 m, mesh size of the PV plate is 9.99e-003 m, and the mesh size of the control volume is as default.

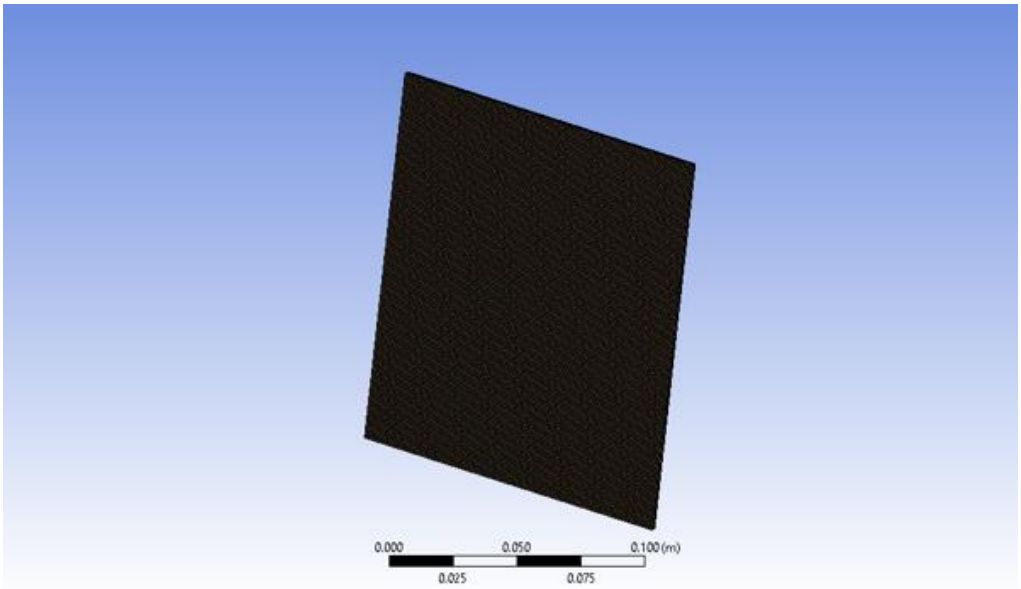

Figure 4.4. Meshing in PV panel

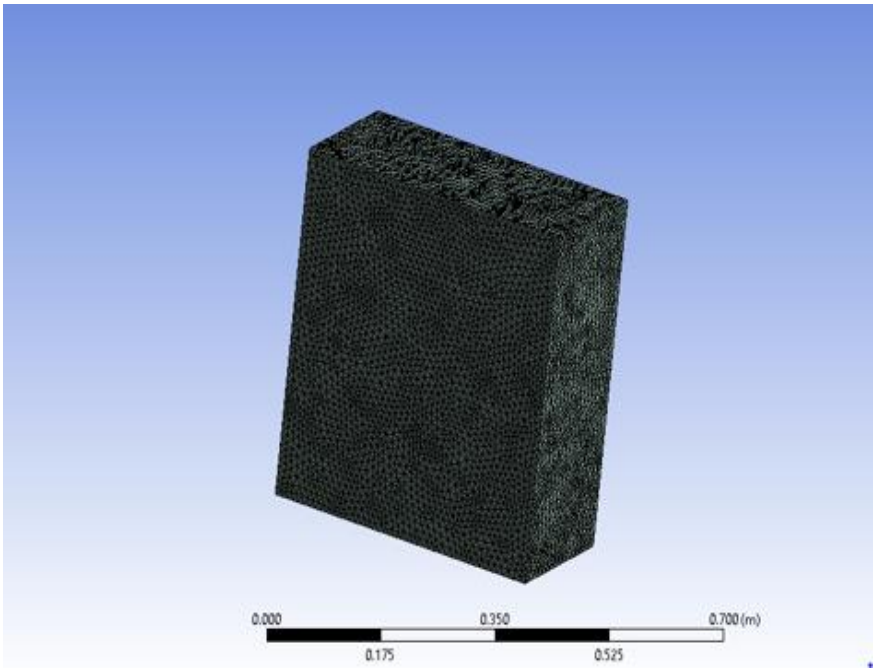

Figure 4.5. Meshing in the problem domain

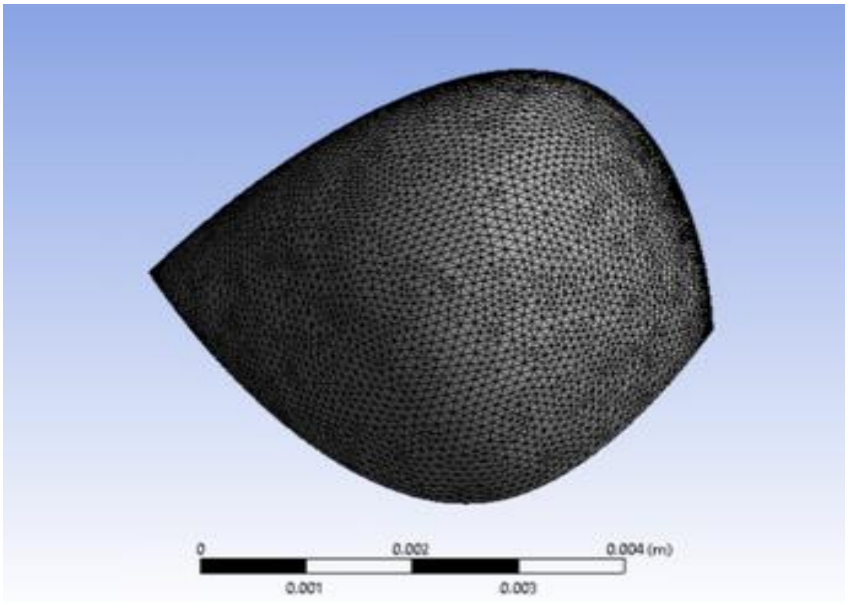

Figure 4.6. Meshing in the droplet

4.2. Solution Method

After meshing is accomplished, the next step is the setup and solution. Basic properties and boundary conditions are assigned in the setup and solution section. Temperature distribution is a function of time and position both. Hence the problem is treated as transient. After selecting the model for simulation process, the next step is choosing the types of material (fluid or solid) and select the material based on the properties. Here, air and water are selected as a fluid material and glass is selected as a solid material. The properties of the water are as shown in the figure below.

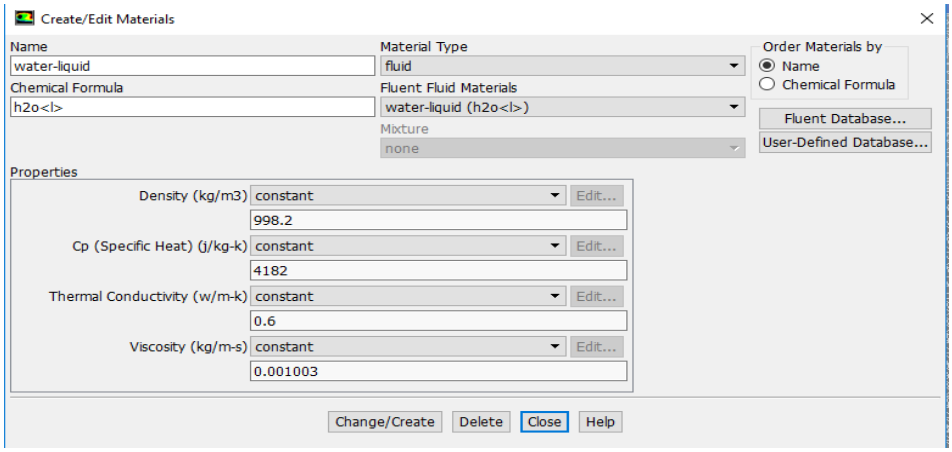

Figure 4.7. Properties of water

The next step is to select the solid material which is the coating over the PV panel. Density of the coating is 2800 kg/m^3 with the specific heat of 910 J/kg-K. Cell-zone of the drop is selected as water, cell-zone of the control volume is selected as air and cell-zone of the PV panel selected as the glass. Time step was selected as 0.001 s for the simulations. At t =0, there is no heat transfer occur between the droplet, solar plate, and the air.

4.3. Boundary Conditions

There are basically two major steps in identifying boundary conditions. First is to define boundary on the design model and second is give the boundary conditions. In this analysis, the default boundary condition is taken into account for each zone and the temperature of each zone (solid, liquid, air) is defined in the patch section. After determining the boundary condition, a mesh interface for the boundary condition defined. When there are different two bodies (water droplet and surface) which do have the same boundary at that time it is required to define a boundary condition interface. The main objective of creating the interface is to assure that there is no transfer of mass between two bodies but there is a transfer of heat that takes place between the two bodies.

CHAPTER 5

RESULTS

In this chapter, numerical analysis of heat transfer between three media (water droplet, PV panel, surrounding air) is described. ANSYS Fluent (R17.2) was used for the analysis. Temperature of the droplet, PV panel and surrounding air were selected as 295 K, 305 K, and 313 K respectively. Table 5.1 below lists the cases studied in this analysis. Results for the PV panel in this study are presented in terms of average panel temperature. As the droplet volumes studied were comparatively small, surface area covered by the droplets on the sample panel was also small. Hence, temperature variations obtained seemed to be low due to the droplet coverage over the PV panel being small. Percent coverage of the droplets for each case is presented in Table 5.2.

Table 5.1. Cases studied for numerical analysis

Droplet volume (µl)	Number of droplets	Distance between droplets (mm)		
30	Single	N/A		
	Two	1.82	3.63	5.5
	Three	1.82	3.63	5.5
60	Single	N/A		
	Two	2.57	5.15	7.9
	Three	2.57	5.15	7.9

Table 5.2. Droplet coverage

Droplet volume (µl)	Number of droplets	Percent coverage (%)
30	Single	0.51
	Two	1.02
	Three	1.53
60	Single	0.82
	Two	1.64
	Three	2.46

30 µl (L = 5.5 mm) single droplet

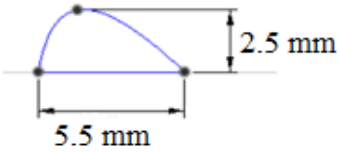

Figure 5.1. Single droplet of 30 µl volume

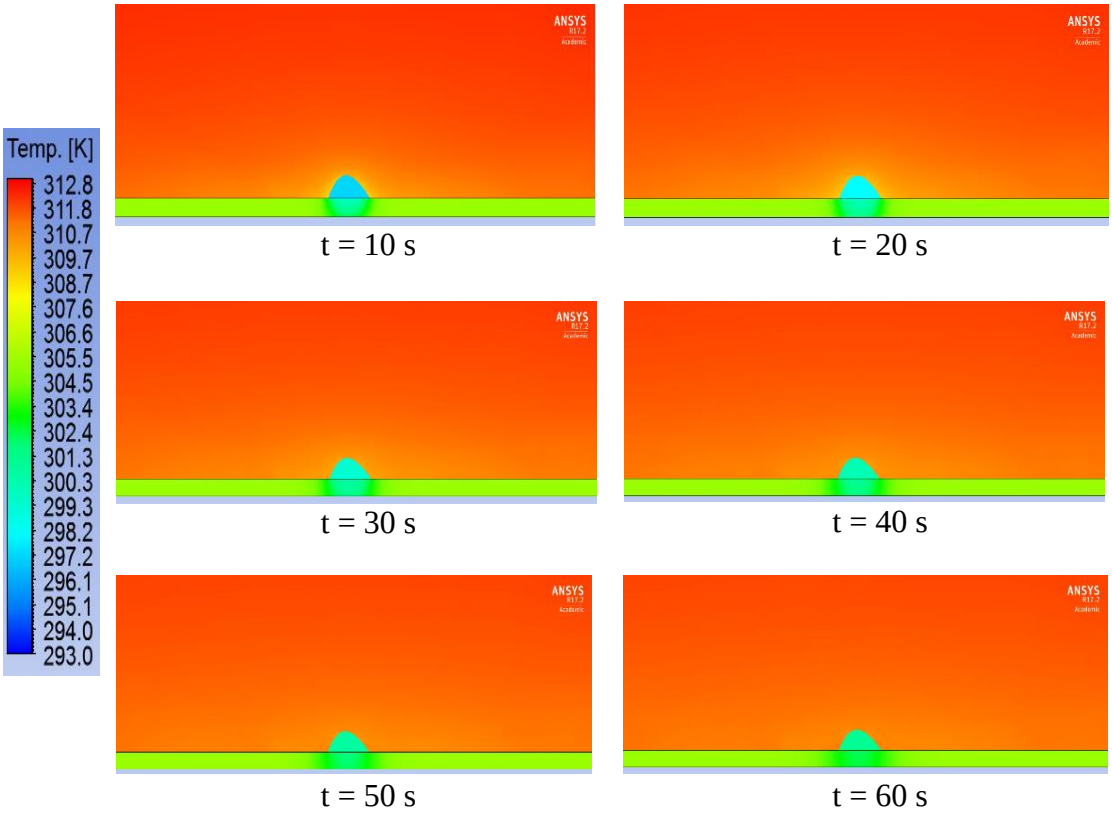

Figure 5.2. Temperature distribution by 30 µl volume of single droplet

30 µl (L = 5.5 mm) two droplets at a distance of 1.81 mm

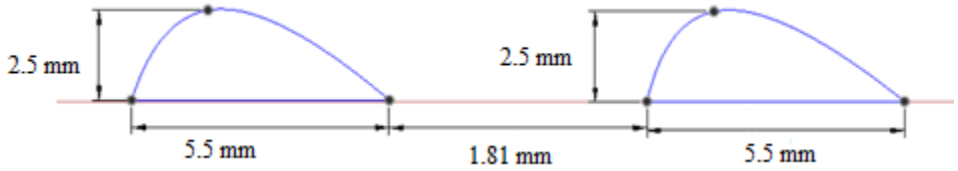

Figure 5.3. Two droplets of volume 30 µl at a distance of 1.81 mm

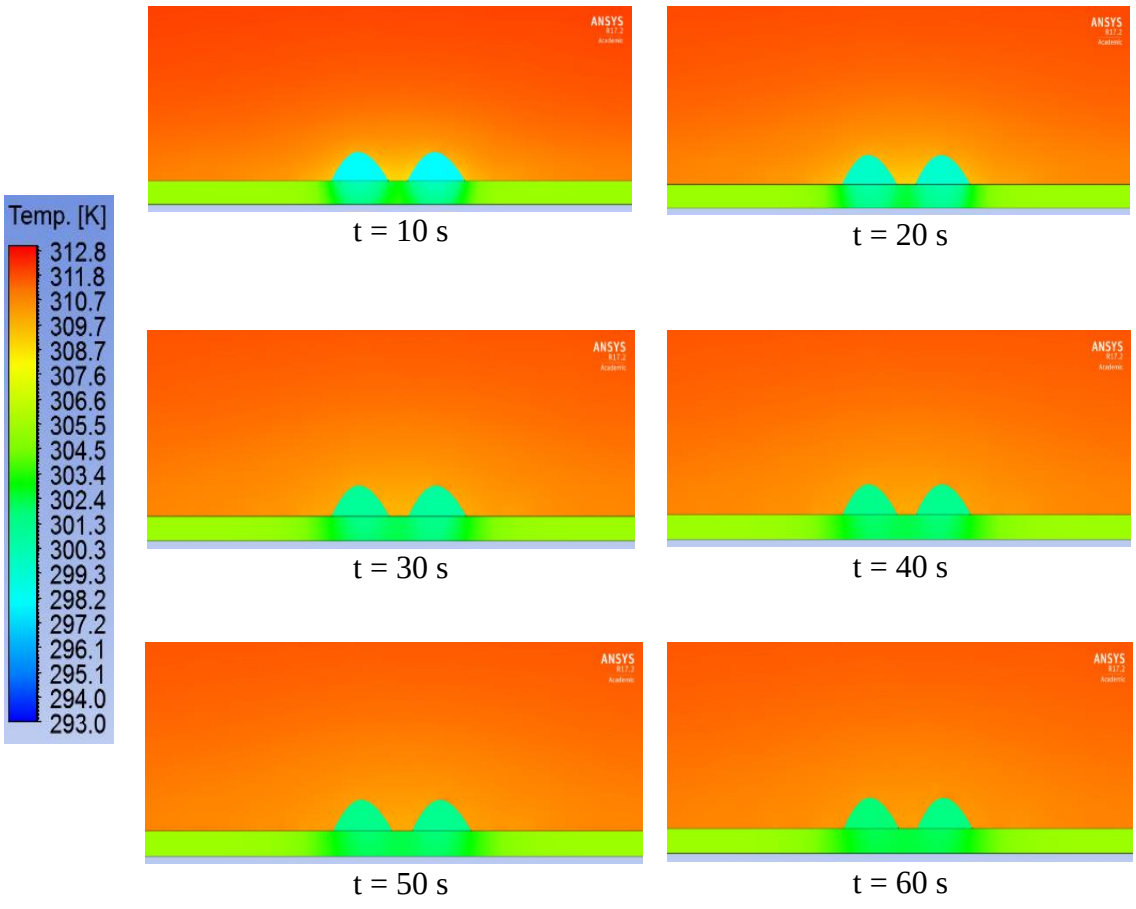

Figure 5.4. Temperature distribution around two 30 µl volume droplets at a distance of 1.81 mm

30 µl (L = 5.5 mm) two droplets at a distance of 3.63 mm

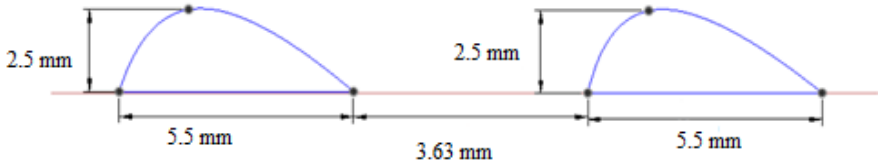

Figure 5.5. Two droplets of 30 µl volume at a distance of 3.63 mm

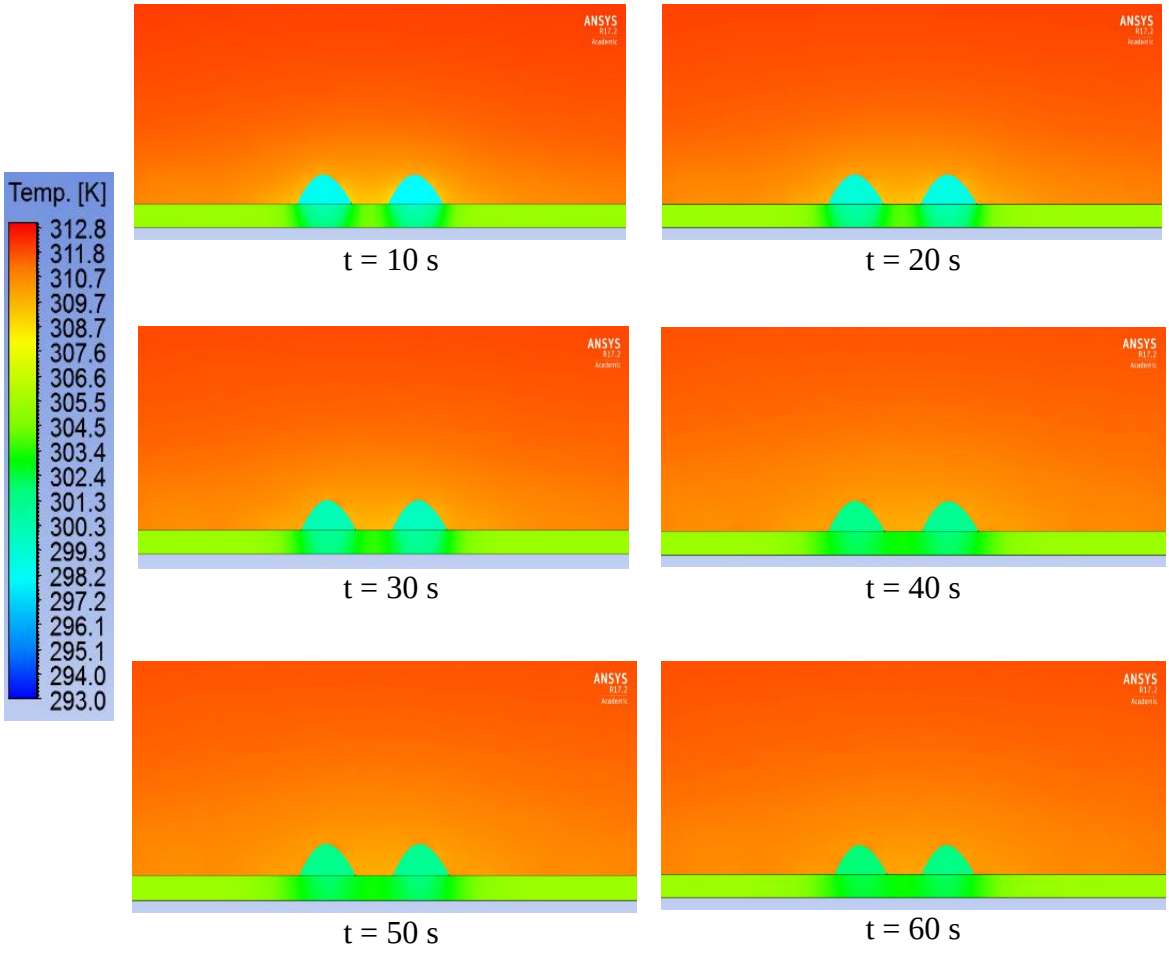

Figure 5.6. Temperature distribution around two 30 µl volume droplets at a distance of 3.63 mm

30 µl (L = 5.5 mm) two droplets at a distance of 5.5 mm

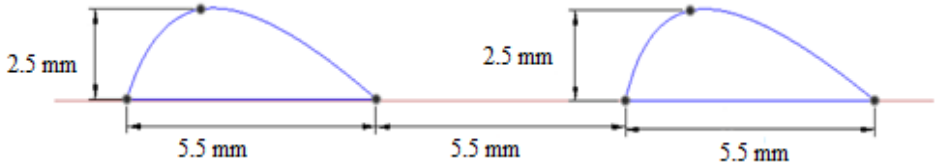

Figure 5.7. Two droplets of 30 µl volume at a distance of 5.5 mm

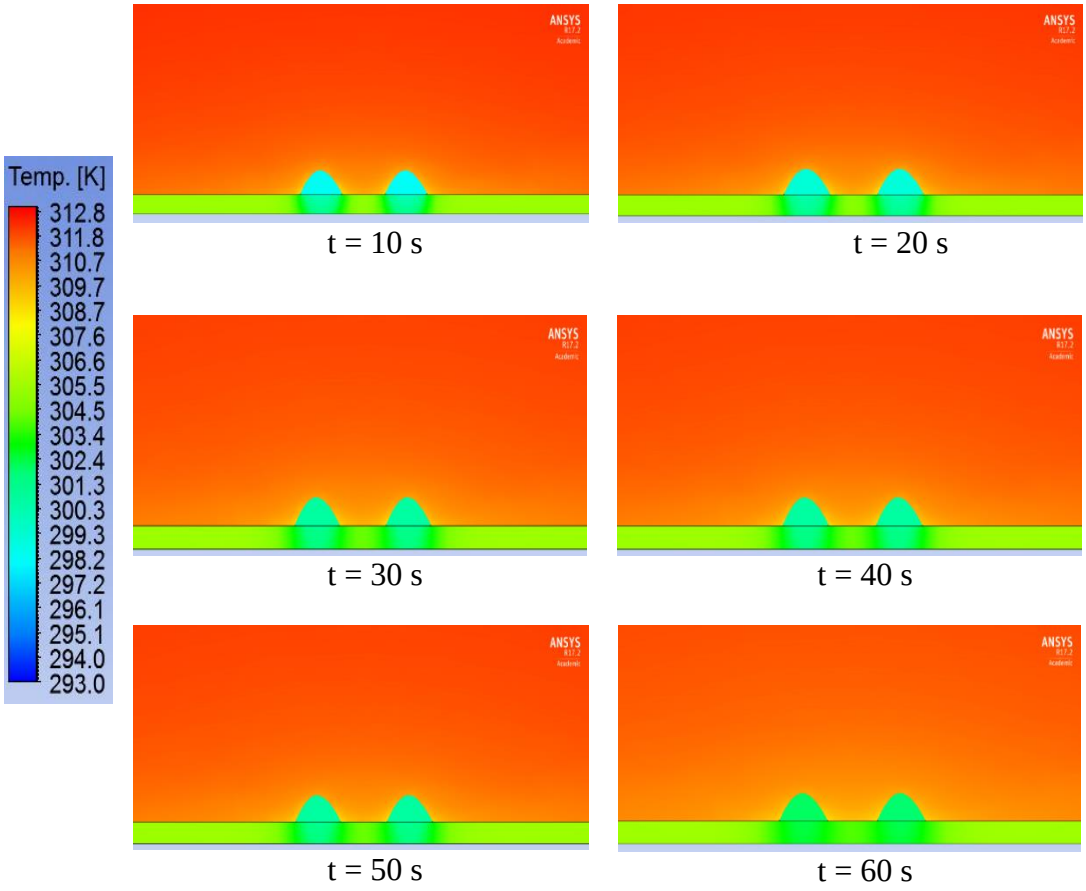

Figure 5.8. Temperature distribution around two 30 µl volume droplets at a distance of 5.5 mm

30 µl three droplets at a distance of 1.81 mm

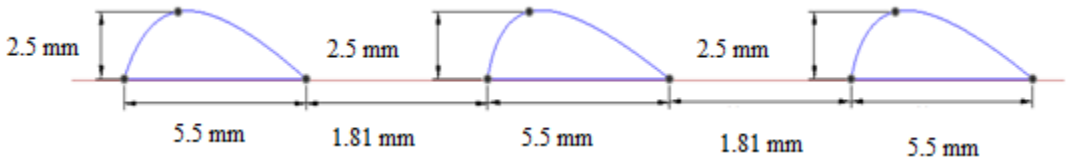

Figure 5.9. Three droplets of 30 µl volume at a distance of 1.81 mm

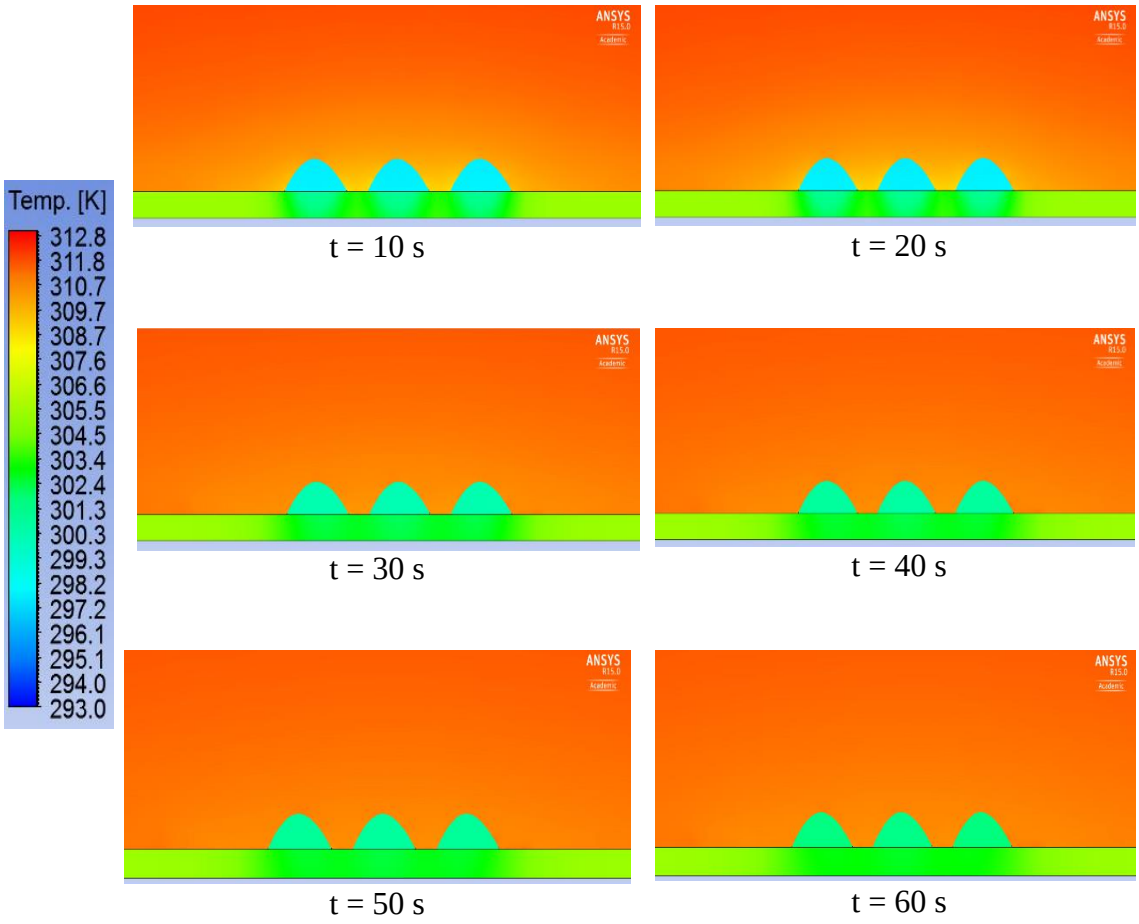

Figure 5.10. Temperature distribution around three 30 µl volume droplets at a distance of 1.81 mm

30 µl three droplets at a distance of 3.63 mm

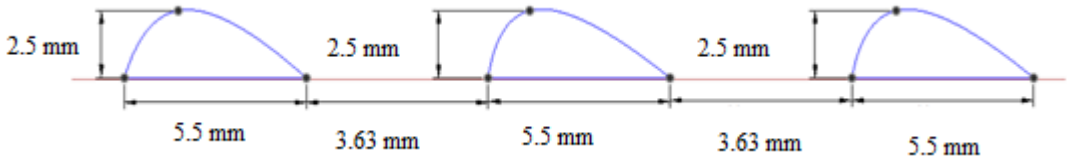

Figure 5.11. Three droplets of 30 µl at a distance of 3.63 mm

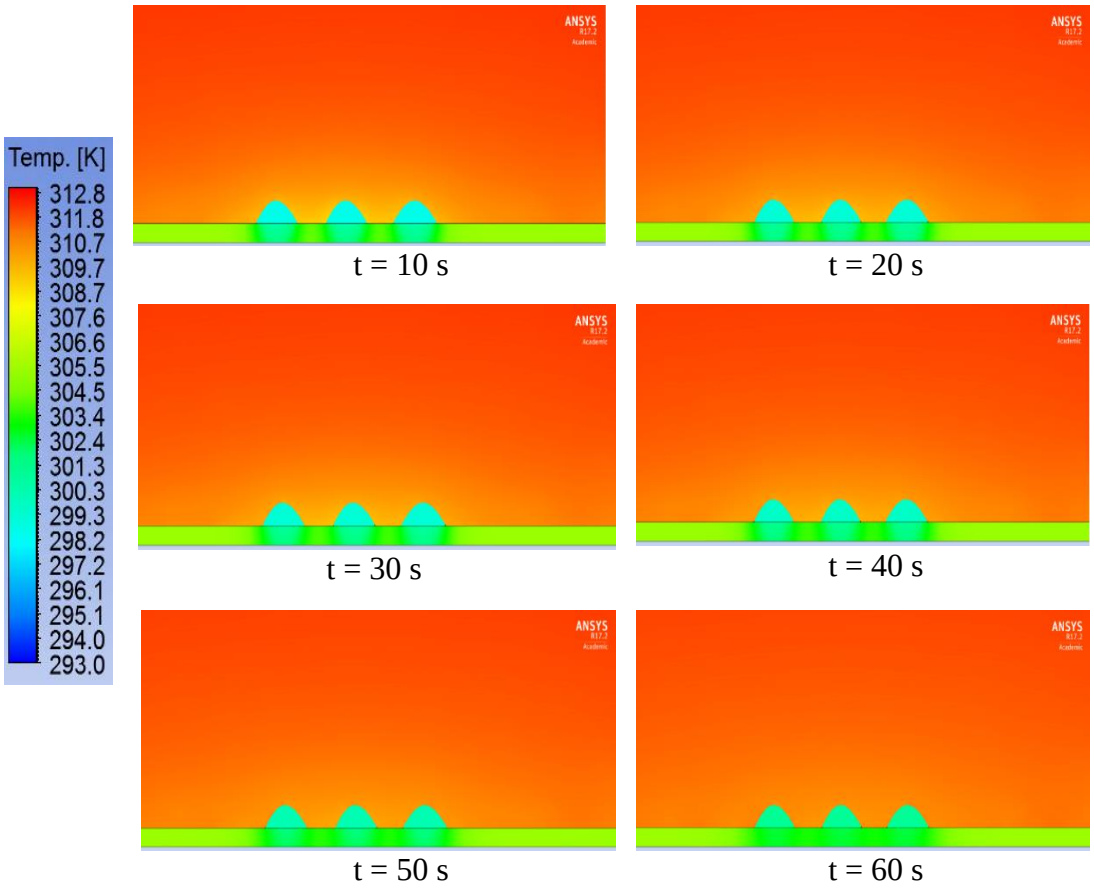

Figure 5.12. Temperature distribution around three 30 µl volume droplets at a distance of 3.63 mm

30 µl three droplets at a distance of 5.5 mm

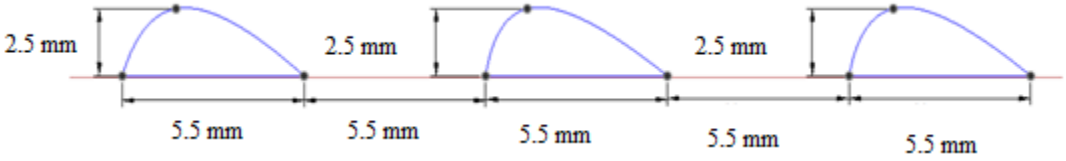

Figure 5.13. Three droplets of 30 µl volume at a distance of 5.5 mm

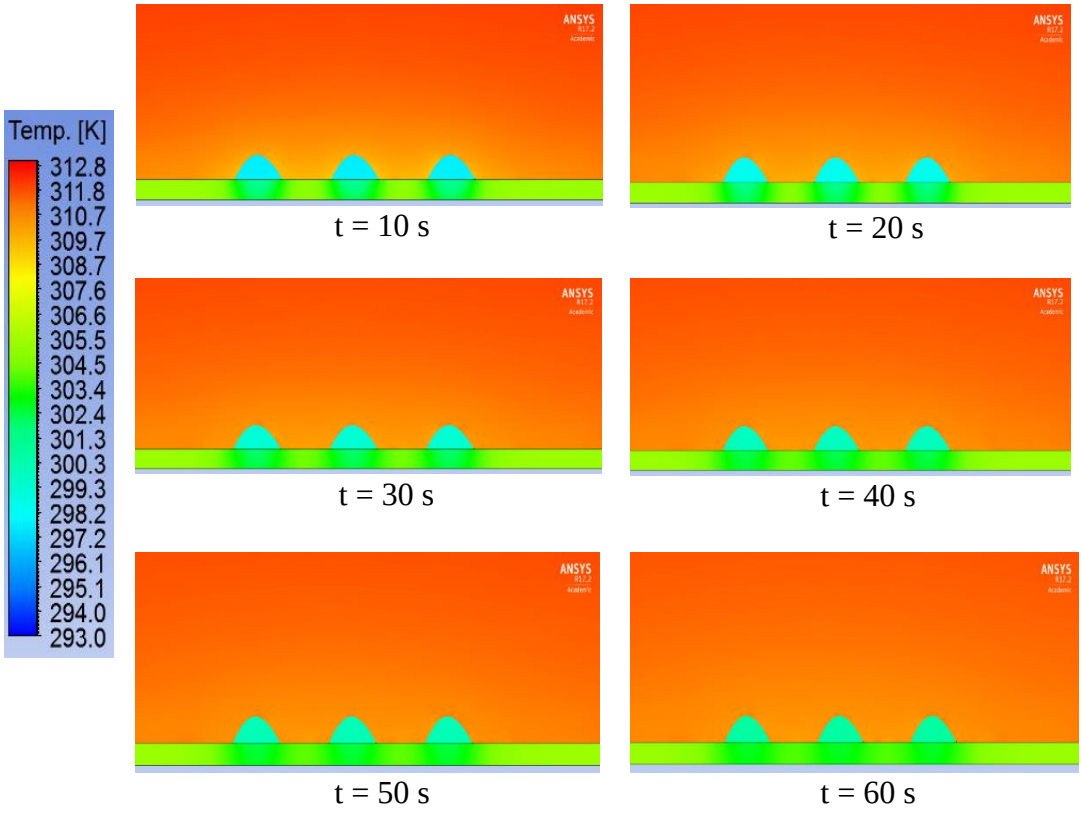

Figure 5.14. Temperature distribution around three 30 µl volume droplets at a distance of 5.5 mm

60 µl (L = 7.9 mm) single droplet

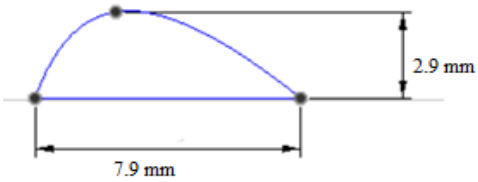

Figure 5.15. Sigle droplet of 60 µl volume

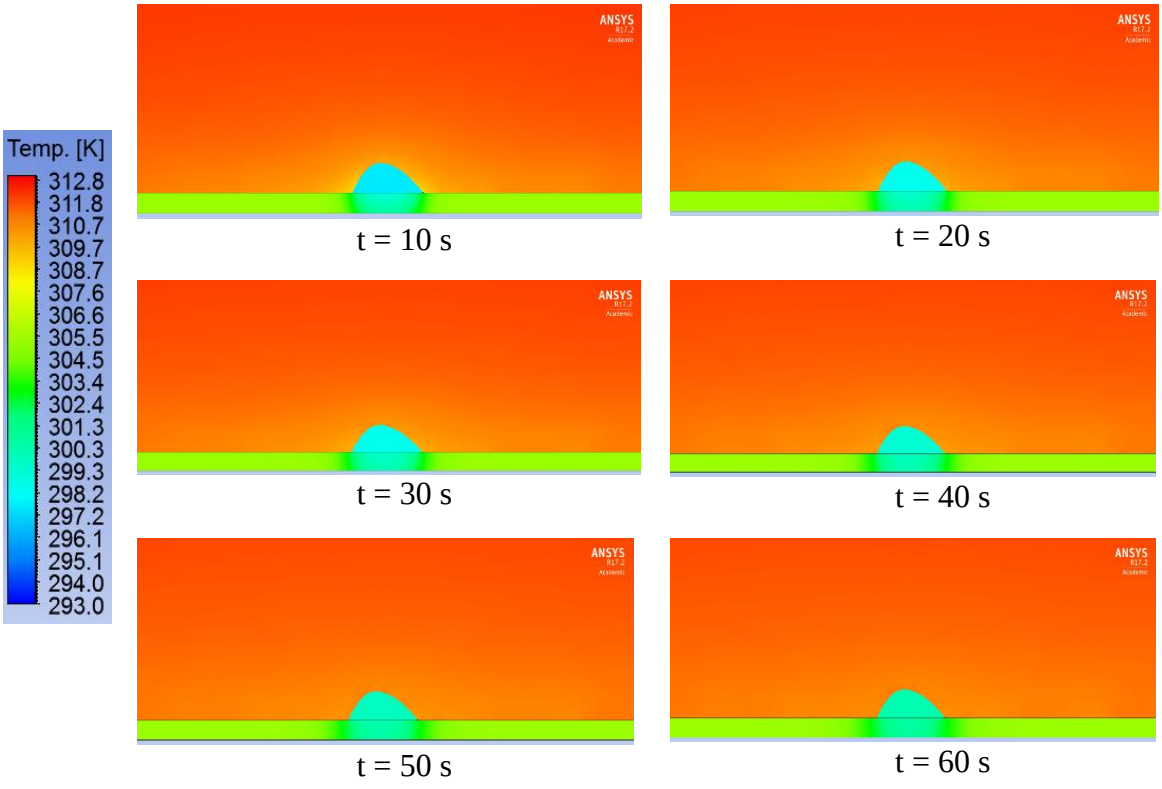

Figure 5.16. Temperature distribution around single 60 µl droplet

60 µl (L = 7.9 mm) two droplets at a distance of 2.57 mm

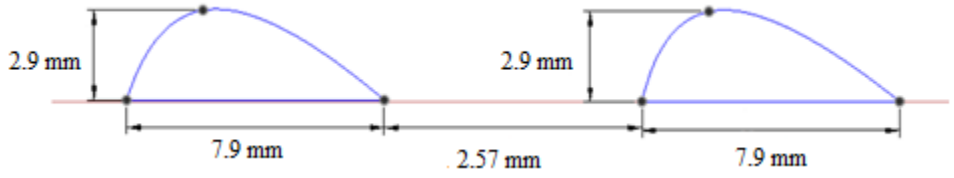

Figure 5.17. Two droplets of 60 µl volume at a distance of 2.57 mm

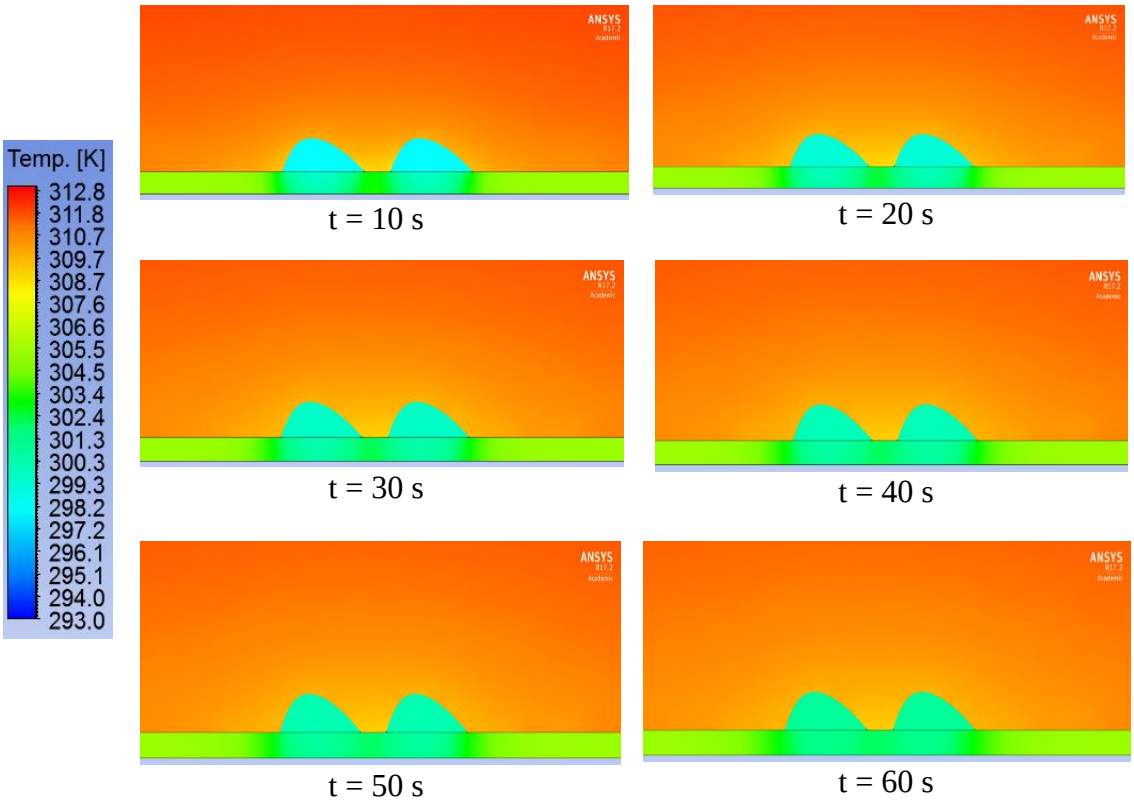

Figure 5.18. Temperature distribution around two 60 µl volume droplets at a distance of 2.57 mm

60 µl (L = 7.9 mm) two droplets at a distance of 5.15 mm

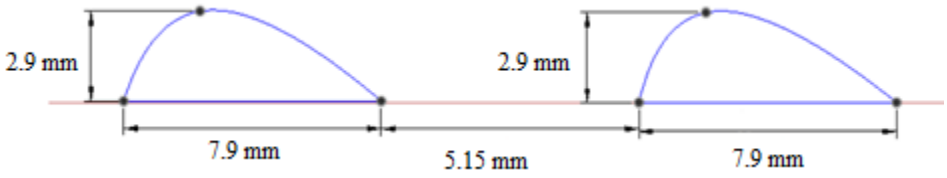

Figure 5.19. Two droplets of 60 µl volume at a distance of 5.15 mm

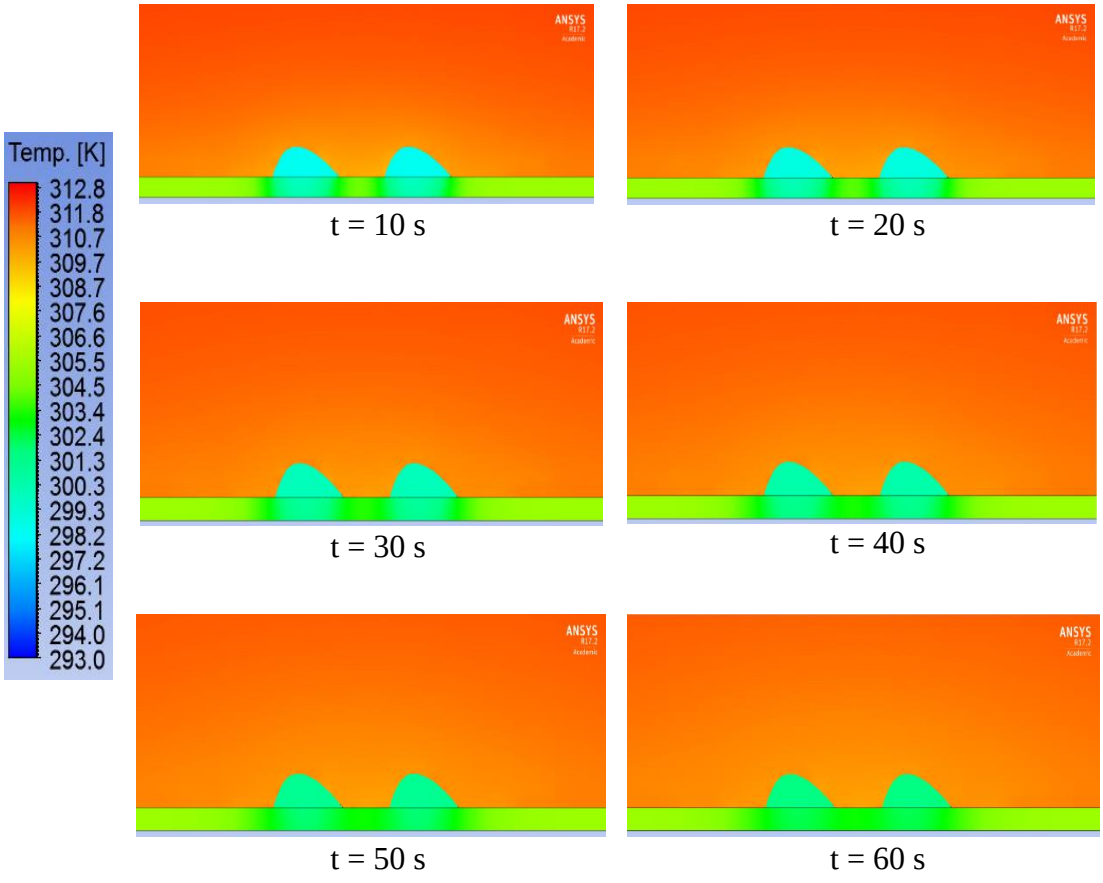

Figure 5.20. Temperature distribution around two 60 µl volume droplets at a distance of 5.15 mm

60 µl (L = 7.9 mm) three droplets at a distance of 7.8 mm

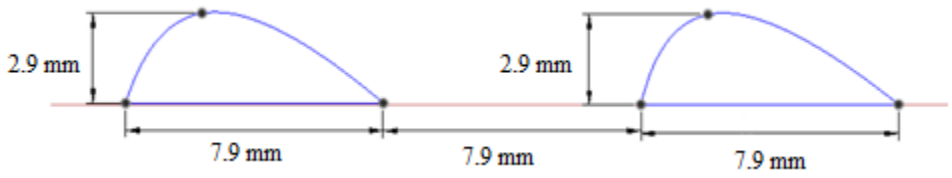

Figure 5.21. Two droplets of 60 µl volume at a distance of 7.9 mm

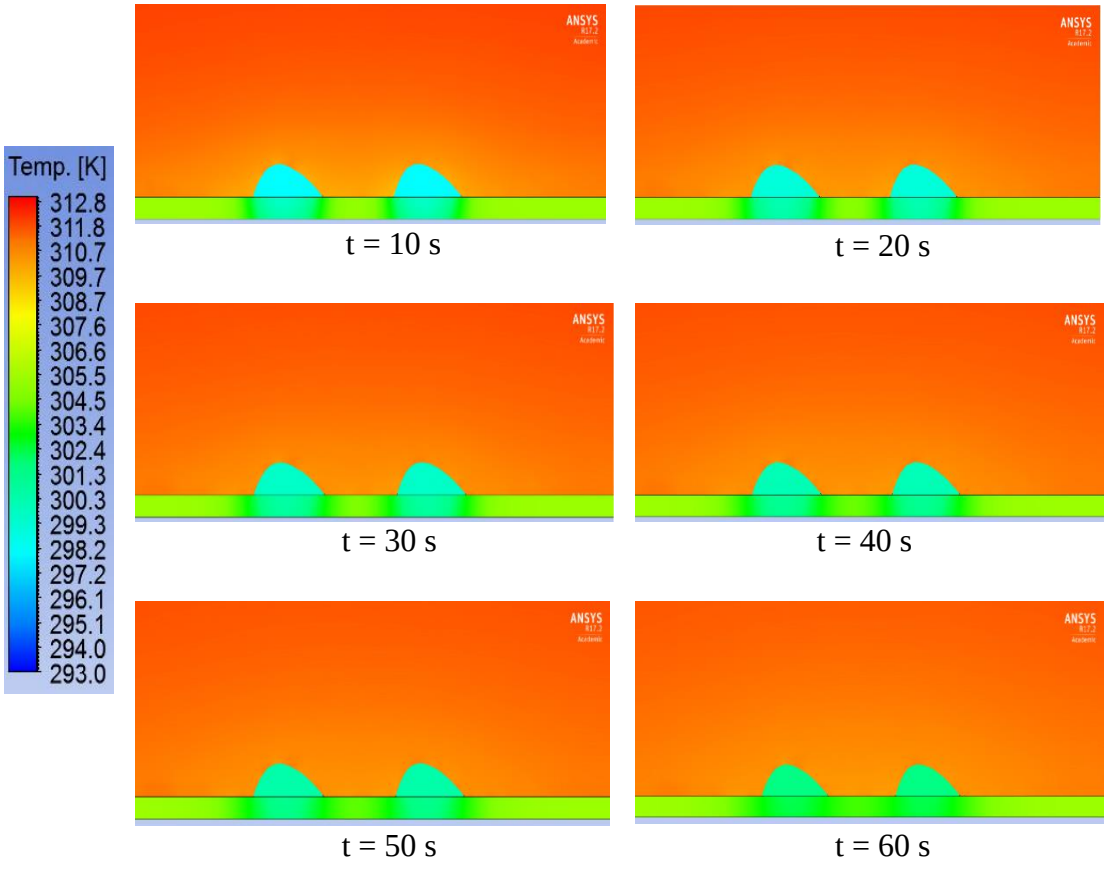

Figure 5.22. Temperature distribution around two 60 µl volume droplets at a distance of 7.9 mm

60 µl (L = 7.9 mm) three droplets at a distance of 2.57 mm

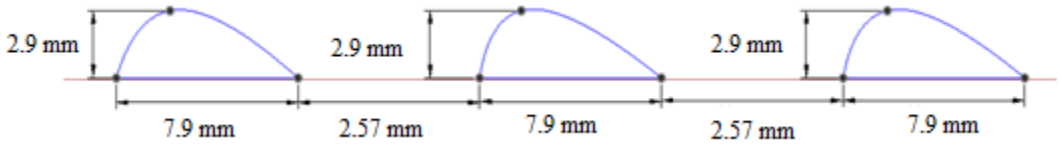

Figure 5.23. Three droplets of 60 µl volume at a distance of 2.57 mm

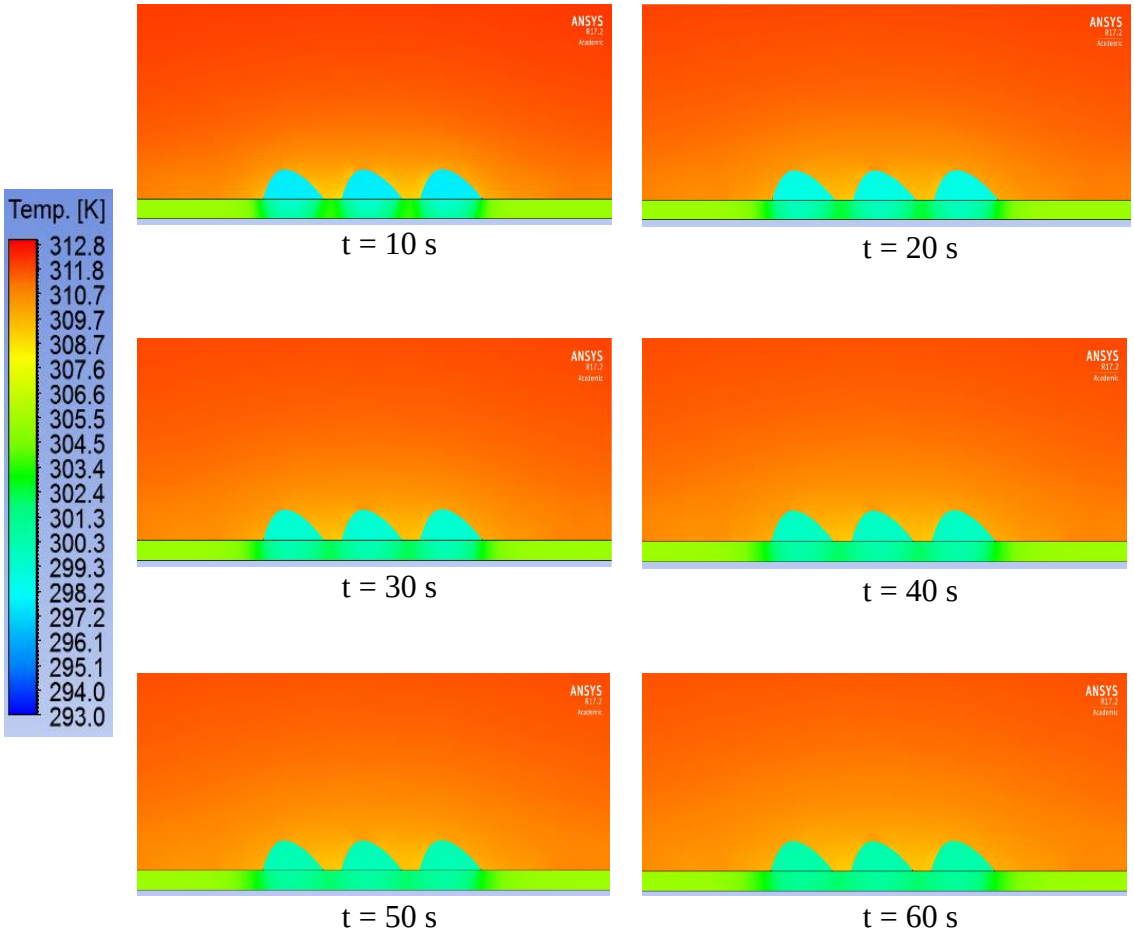

Figure 5.24. Temperature distribution around three 60 µl volume droplets at a distance of 2.57 mm

60 µl (L = 7.9 mm) three droplets at a distance of 5.15 mm

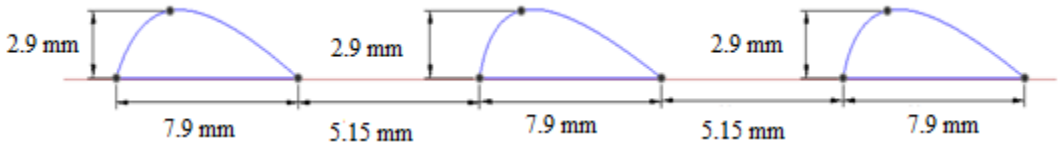

Figure 5.25. Three droplets of 60 µl volume at a distance of 5.15 mm

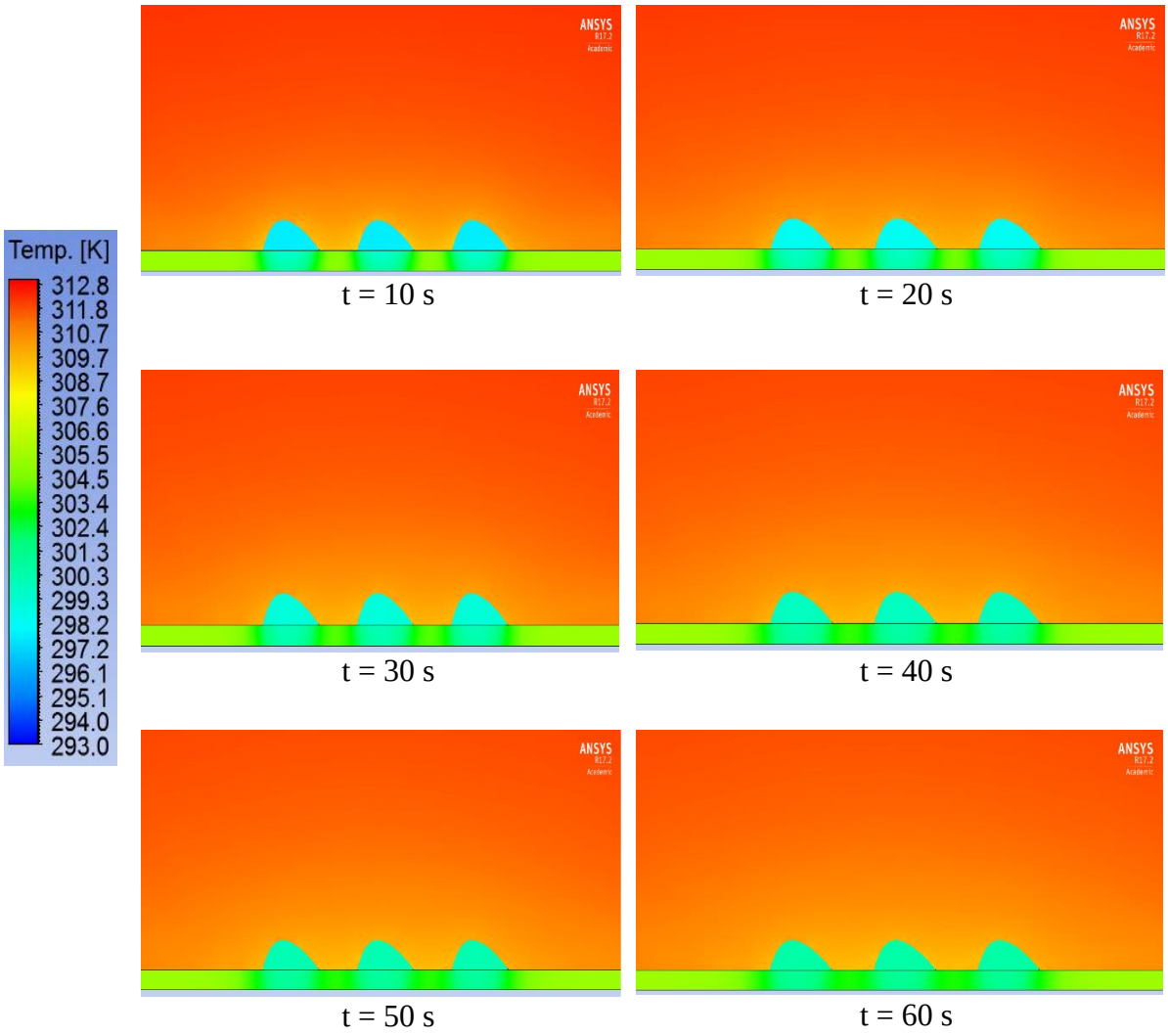

Figure 5.26. Temperature distribution around three 60 µl volume droplets at a distance of 5.15 mm

60 µl (L = 7.9 mm) three droplets at a distance of 7.9 mm

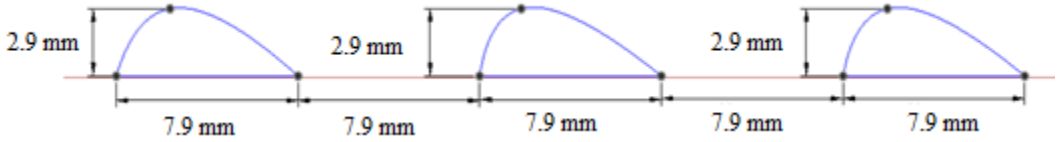

Figure 5.27. Three droplets of 60 µl at a distance of 7.9 mm

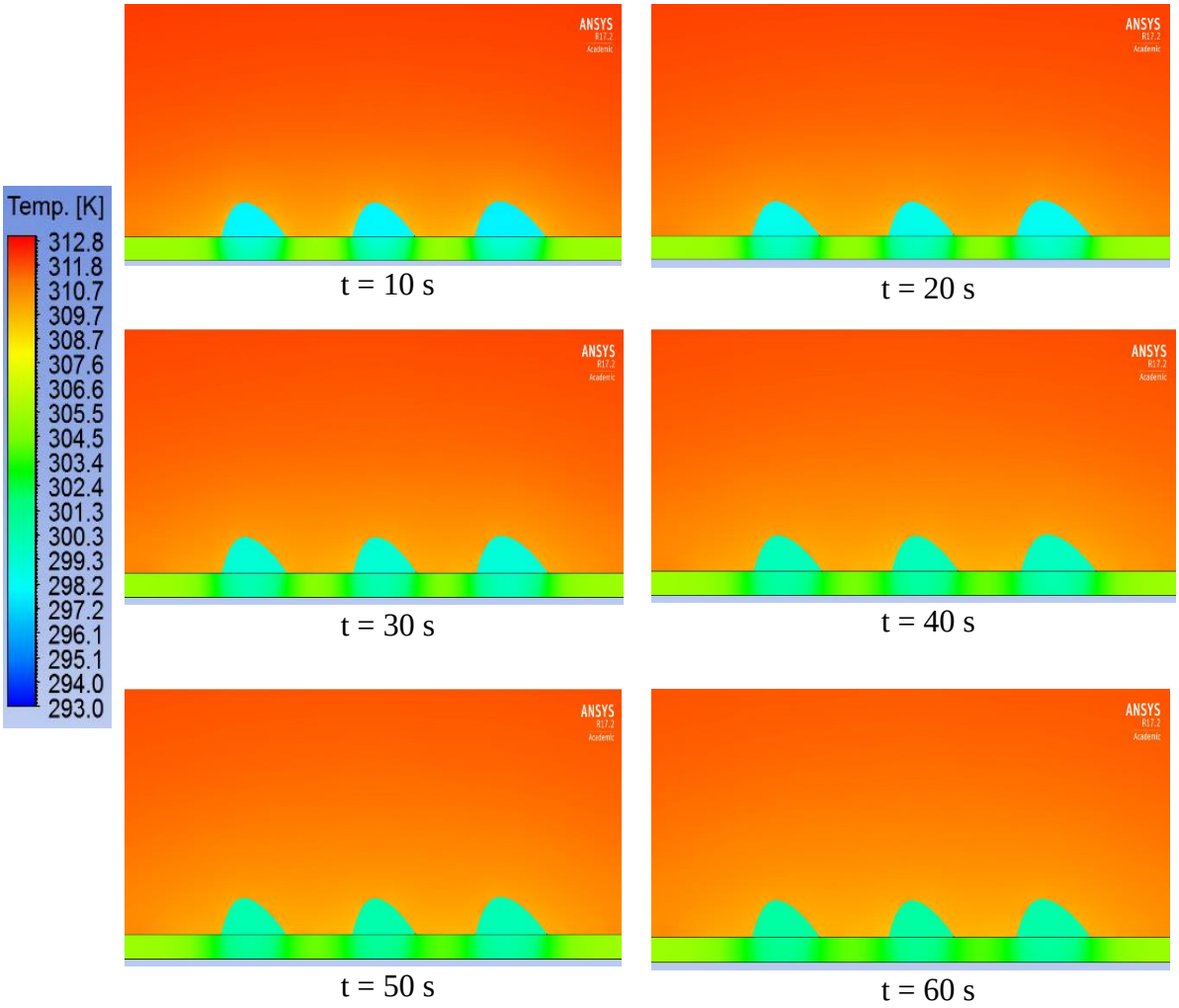

Figure 5.28. Temperature distribution around three 60 µl droplets at a distance of 7.9 mm

Temperature behavior of the different cases analyzed hence been plotted for various comparison criteria in Figures 5.29-35.

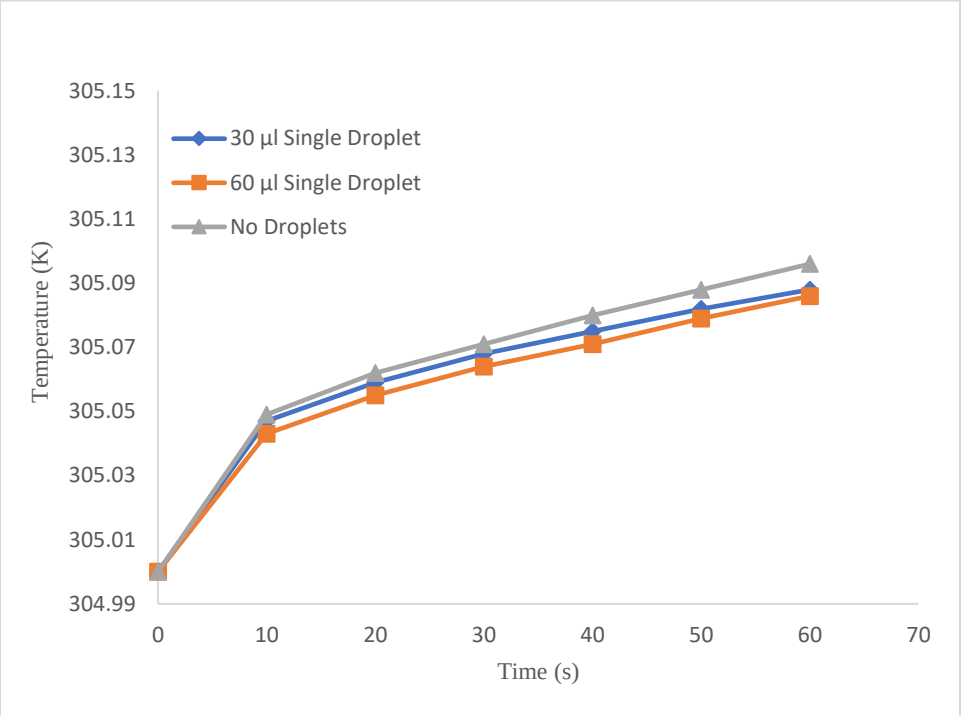

Figure 5.29. Temperature variation of dry panel surface vs wetted with different droplet volumes

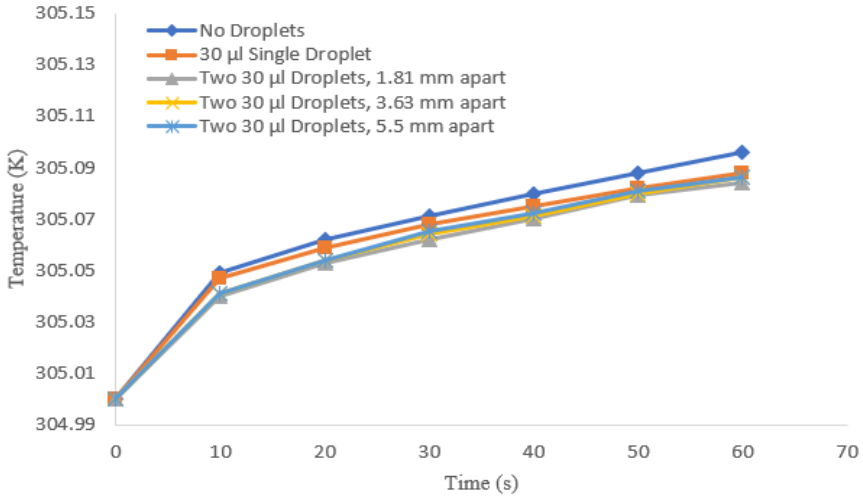

Figure 5.30. Temperature variation of PV panel under different droplet distances (two 30 µl droplets)

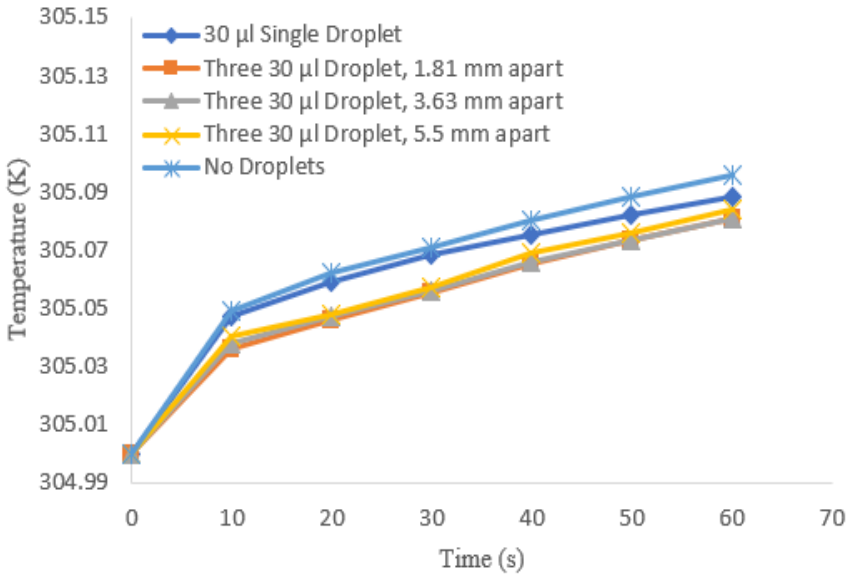

Figure 5.31. Temperature variation of PV panel under different droplet distances (three 30 µl droplets)

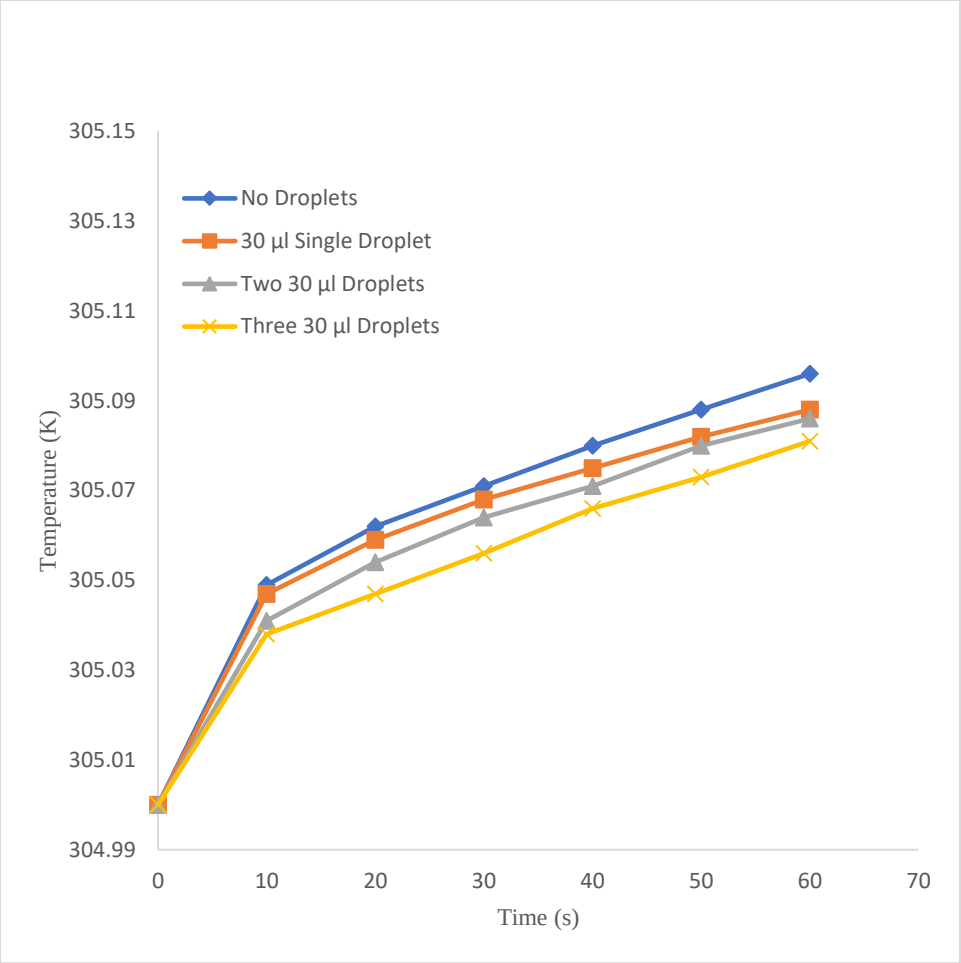

Figure 5.32. Temperature variation of PV panel under different number of 30 µl droplets

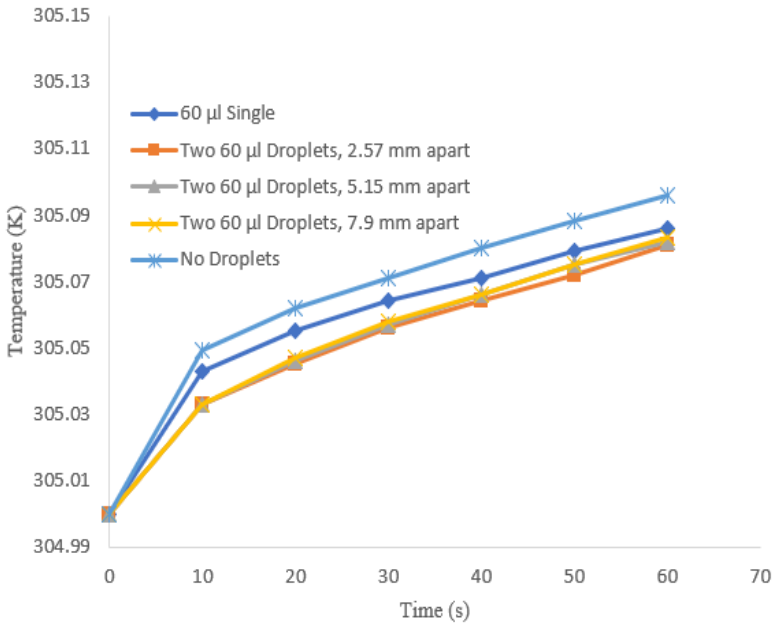

Figure 5.33. Temperature variation of PV panel under different droplet distances (two 60 µl droplets)

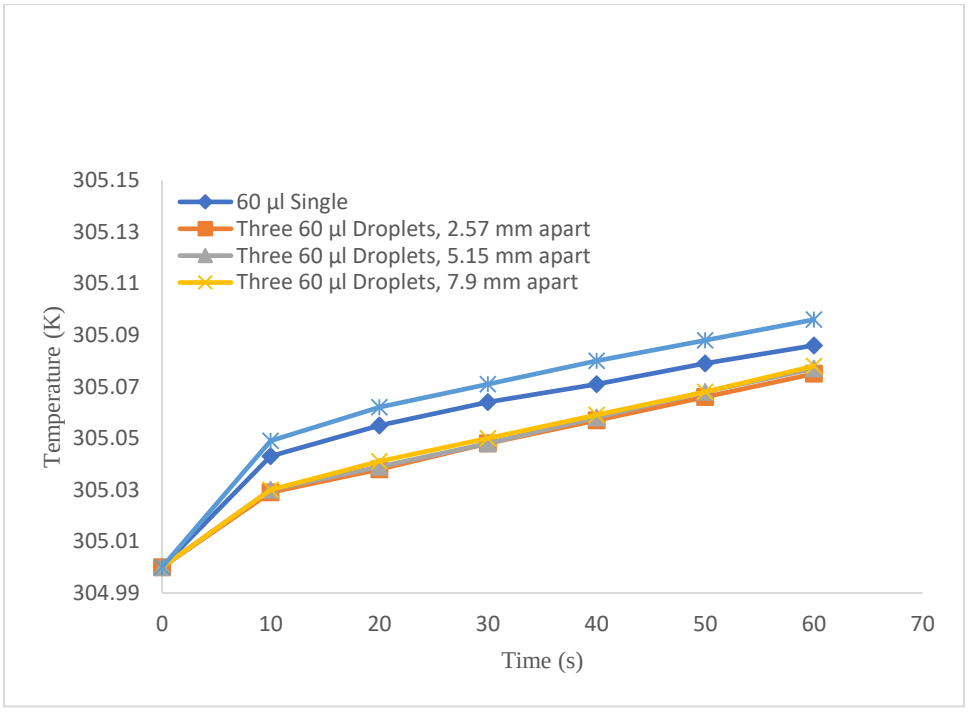

Figure 5.34. Temperature variation of PV panel under different droplet distances (three 60 µl droplets)

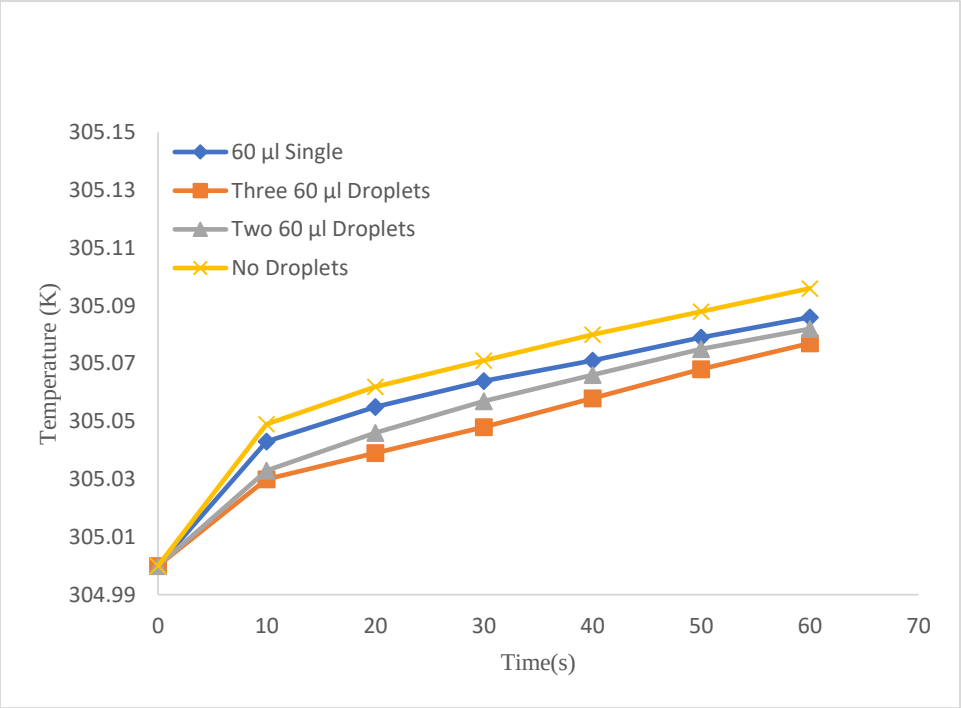

Figure 5.35. Temperature variation of PV panel under different number of 60 µl droplets

CHAPTER 6

CONCLUSION

Thermal effects of water droplets on PV panel surfaces was investigated in this thesis study. Motivation of this work is fact that energy conversion performance of PV panel increase with decreased PV cell temperature. Hence, quantifying the cooling effect on the PV panel surfaces can help operate these panels at optimal temperature conditions. For the cooling effect of a droplet on the PV panel to be studied, first the relation of a droplet on the inclined surface was assured theoretically. Then, the het transfer performance between the droplet and the PV panel was studied both theoretically and numerically. The study was conducted at two different droplet volume 60 µl and 30 µl, and for single, two, and three droplet cases at different. For the multiple droplet scenarios, three different distances between the droplets were analyzed. The findings of this study can be listed as follows.

- Droplet retention on PV panel surface after a rain, condensation or irrigation event is observed when the drag force dominates the body forces.
- Amount of heat transfer increases with increasing droplet volume and contact area. Hence more heat transfer is observed over hydrophilic surfaces then hydrophobic surfaces.
- As the number of droplets over the PV panel surface increase, cell temperature decrease which would yield panel efficiency.
- It was observed that as the distance between the droplets increases, cooling effect lessens. This decrease in the cooling effect would get higher as the droplets get further away from each other.

As for the future recommendations based on the findings of this study, it is suggested that the thermal effects of water droplets are studied combined with the optical effects so that the problem is analyzed with a wider perspective.

REFERENCES

[1] M. Khaled, M.S. Abd-Elhady, H.A. Kandil, and H. Sherif. "Enhancing the performance of photovoltaic panels by water cooling" *Ain Shams Engineering Journal* 4, no. 4 (Dec 1, 2013): 869-877.

[2] A.D Jones, and C.P. Underwood. "A thermal model for photovoltaic systems" *Solar Energy* 70, no. 4 (Jan 1, 2001): 349-359.

[3] *Solar Electric Supply, Inc*. 2017. <https://www.solarelectricsupply.com/bp-solar-bp380j-solar-panels-278>.

[4] Wadud, A.M. Abu, T. Zaman, F. Rabbee, and R. Rahman. "Renewable energy, an ideal solution of energy crisis and economical development in Bangladesh" *Global Journal of Research in Engineering* 13, no. 15 (Dec 31, 2013): 19-28.

[5] S. Dubey, J.N.Sarvaiya, and B.Seshadri. "Temperature dependent photovoltaic (PV) efficiency and its effect on PV production in the world–a review" *Energy Procedia* 33 (Jan 1, 2013): 311-321.

[6] D.M. Tobnaghi, R. Mostafa, R. Madatov, and D. Naderi. "The effect of temperature on electrical parameters of solar cells" *International Journal of Advanced Research in Electrical, Electronics and Instrumentation Engineering* 2, no. 12 (Dec 2, 2013): 6404-6407.

[7] Popovici, C. George, S.V. Hudişteanu, T.D. Mateescu, and N. Chereches. "Efficiency improvement of photovoltaic panels by using air cooled heat sinks" *Energy Procedia* 85 (Jan 1, 2016): 425-432.

[8] Stritih, Uroš. "Increasing the efficiency of PV panel with the use of PCM" *Renewable Energy* 97 (Nov 1, 2016): 671-679.

[9] V. Poulek, A. Khudysh, and M. Libra. "Innovative low concentration PV systems with bifacial solar panels" *Solar Energy* 120 (Oct 1, 2015): 113-116.

[10] S. Matias, C. Abrenhosa, L. Moraes, Santos, A.J. Alves, and W.P. Calixto. "Electrical performance evaluation of PV panel through water cooling technique" In *Environment and Electrical Engineering (EEEIC), IEEE 16th International Conference*, IEEE (June 7, 2016) pp. 1-5.

[11] K. Moharram, A. Khaled, M.S. Abd-Elhady, H.A. Kandil, and H. Sherif. "Enhancing the performance of photovoltaic panels by water cooling" *Ain Shams Engineering Journal* 4, no. 4 (Dec 1, 2013): 869-877.

[12] G.N. Tiwari, S. Tiwari, V.K. Dwivedi, S. Sharma, and V. Tiwari. "Effect of water flow on PV module: A case study" In *Energy Economics and Environment (ICEEE), International Conference*, (March 27, 2015) pp. 1-7. IEEE.

[13] Kim, Ho-Young, H.J. Lee, and B.H. Kang. "Sliding of liquid drops down an inclined solid surface" *Journal of Colloid and Interface Science* 247, no. 2 (March 15, 2002): 372-380.

[14] D. Qingwen, M.M. Khonsari, C. Shen, W. Huang, and X. Wang. "On the migration of a droplet on an incline" *Journal of colloid and interface science* 494 (May 15, 2017): 8-14.

[15] T. Maurer, A. Mebus, and U. Janoske. "water droplet motion on an inclining surface" In *Proceedings of the 3rd International Conference on Fluid Flow, Heat and Mass Transfer (FFHMT'16), Ottawa, Canada–May 2*, pp. 2-3. 2016.

[16] Quéré, David, Marie-José Azzopardi, and Laurent Delattre. "Drops at rest on a tilted plane" *Langmuir* 14, no. 8 (Apr 14, 1998): 2213-2216.

[17] Kim, H. Young, H.J. Lee, and B. Kang. "Sliding of liquid drops down an inclined solid surface" *Journal of colloid and interface science* 247, no. 2 (March 15, 2002): 372-380.

[18] M.J. Santos, S. Velasco, and J. A. White. "Simulation analysis of contact angles and retention forces of liquid drops on inclined surfaces" *Langmuir* 28, no. 32 (Aug 3, 2012): 11819-11826.

[19] D. Quéré and M. Reyssat. "Non-adhesive lotus and other hydrophobic materials" *Philosophical Transactions of the Royal Society of London A: Mathematical, Physical and Engineering Sciences* 366, no. 1870 (May 13, 2008): 1539-1556.

[20] B. Bhushan, M. Nosonovsky, and Y.C Jung. "Towards optimization of patterned superhydrophobic surfaces" *Journal of the Royal Society Interface* 4, no. 15 (Aug 22, 2007): 643-648.

[21] N. Nakata, M. Kakimoto, and T. Nishita 2012. "Animation of water droplets on a hydrophobic windshield" *Proc. 20th Int. Conf. Comput. Graphics, Visualization and Comput. Vision* (Jun 15, 2012)

[22] *The Dry Drops on Folien 1*. 2013. 2013. http://www.justice4inge.com/Dry_drops_report_web_low.pdf

[23] R. Annapragada, J.Y.Murthy, and V.G. Suresh. "Droplet retention on an incline" *International Journal of Heat and Mass Transfer* 55, no. 5-6 (Feb 1, 2012): 1457-1465.

[24] A. Sommers and M.A. Jacobi, "Calculating the volume of water droplets on topographically-modified, micro-grooved aluminum surfaces" (July 14, 2008). *International Refrigeration and Air Conditioning Conference*. Paper 931: 2282(1-8).

[25] S. Chavan, H. Cha, D. Orejon, K. Nawaz, N. Singla, Y.F. Yeung, D. Park. "Heat transfer through a condensate droplet on hydrophobic and nanostructured superhydrophobic surfaces" *Langmuir* 32, no. 31 (Jul 28, 2016): 7774-7787.